Copyright Warning & Restrictions

The copyright law of the United States (Title 17, United States Code) governs the making of photocopies or other reproductions of copyrighted material.

Under certain conditions specified in the law, libraries and archives are authorized to furnish a photocopy or other reproduction. One of these specified conditions is that the photocopy or reproduction is not to be "used for any purpose other than private study, scholarship, or research." If a, user makes a request for, or later uses, a photocopy or reproduction for purposes in excess of "fair use" that user may be liable for copyright infringement,

This institution reserves the right to refuse to accept a copying order if, in its judgment, fulfillment of the order would involve violation of copyright law.

Please Note: The author retains the copyright while the New Jersey Institute of Technology reserves the right to distribute this thesis or dissertation

Printing note: If you do not wish to print this page, then select "Pages from: first page # to: last page #" on the print dialog screen

ABSTRACT

DIFFUSE AXONAL INJURY EFFECT ON MYELINATING CELLS AND AXONS

by
Jennifer Alison Zalk

There is no supporting evidence whether myelin degeneration in diffuse axonal injury (DAI) of the white matter is due to death of myelinating oligodendrocytes or secondary axotomy. Cortical neurons are not able to remain healthy in culture to have their axons myelinated. Dorsal root ganglion (DRG) neurons have been shown to be myelinated by cortical oligodendrocytes in culture. An *in vit*ro stretch injury model was used to analyze the DRG axon pathology during and after injury. DRG myelinating Schwann cells are analyzed to demonstrate what is expected from injury to oligodendrocytes. DRG axons demonstrated a high tolerance to stretch injury compared to cortical axons, at strains up to 90% without disconnection. Axons showed delayed recovery of the developed distortions from injury to their preinjured orientation. Injured DRG axons developed swellings similar to those found along stretch injured cortical axons and in humans with DAI. The intracellular calcium level showed extracellular entry of calcium during injury and high sustained levels following a severe injury. Undifferentiated Schwann cells showed greater calcium influx from severe injury and the possible release of an extracellular signaling molecule increasing the calcium concentration in uninjured cells. Stretch injured differentiated Schwann cells demonstrated an increase in intracellular calcium at the time of injury and a gradual increase in non-injured cells after injury, possibly induced by extracellular signaling molecules and calcium ions traversing to non-injured cells through gap junctions.

DIFFUSE AXONAL INJURY EFFECT ON MYELINATING CELLS AND AXONS

by
Jennifer Alison Zalk

A Thesis
Submitted to the Faculty of
New Jersey Institute of Technology
in Partial Fulfillment of the Requirements for the Degree of
Master of Science in Biomedical Engineering

Department of Biomedical Engineering

January 2013

APPROVAL PAGE

DIFFUSE AXONAL INJURY EFFECT ON MYELINATING CELLS AND AXONS

Jennifer Alison Zalk

Dr. Bryan J. Pfister, Thesis Advisor — Date
Associate Professor of Biomedical Engineering, NJIT

Dr. Haesun Kim, Thesis Co-Advisor — Date
Associate Professor of Biological Sciences, Rutgers

Dr. George Collins, Committee Member — Date
Research Professor of Biomedical Engineering, NJIT

Dr. Cheul H. Cho, Committee Member — Date
Assistant Professor of Biomedical Engineering, NJIT

BIOGRAPHICAL SKETCH

Author: Jennifer Alison Zalk

Degree: Master of Science

Date: January 2013

Undergraduate and Graduate Education:

- Master of Science in Biomedical Engineering,
  New Jersey Institute of Technology, Newark, New Jersey, 2013

- Master of Science in Chemistry,
  Rutgers University, New Brunswick, New Jersey, 2009

- Bachelor of Science in Chemistry,
  Fairleigh Dickinson University, Madison, New Jersey, 2007

Major: Biomedical Engineering

To my parents, Felice R. Zalk and Glenn A. Zalk and brother, Andrew S. Zalk,
Thank you for your support.

ACKNOWLEDGMENT

I sincerely thank the guidance and support from my Thesis Advisor, Dr. Bryan J. Pfister and Co-Advisor, Dr. Haesun Kim. It was a much appreciated opportunity to work with the both of you and to have acquired the knowledge and skills from this research. Thank you to Dr. George Collins and Dr. Cheul H. Cho for being on my Thesis Committee. Thank you to the NJ Commission of Brain Injury for supporting me in this research.

Thank you to Sita Damaraju for your overall help, I sincerely appreciate everything. Thank you to Raj Jaswal for your support and encouragement. Thank you to George Magou and other students in Dr. Pfister's lab. Thank you to the students from Dr. Kim's lab at Rutgers University.

I would like to thank my parents. I will always be indebted to you and appreciate everything. Also thank you to my family, friends and others not mentioned, for your encouragement and help throughout my educational experience.

.

TABLE OF CONTENTS

Chapter **Page**

1 INTRODUCTION……..……..…… 1

1.1 Brain Trauma.……..……...……..……..... 1

1.2 Diffuse Axonal injury.…….…….…….…..... 2

1.3 Myelinated Axon Response to DAI *In Vivo*…...……... 3

1.3.1 Axon Response to DAI……... 3

1.3.2 Myelin Response to DAI…… 4

1.4 DAI *In Vitro*….……..……... 5

1.4.1 *In Vitro* Injury Model……..…… 5

1.5 *In Vitro* Stretch Injury Model..….……. 6

1.5.1 Axonal Response to Stretch Injury Model…….. 6

1.5.2 Myelinated Axon Response to Stretch Injury Model……. 8

1.6 Myelinated Axon Studies…….. 8

1.6.1 Oligodendrocytes Response to TBI…… 9

1.6.2 Calcium Response in Oligodendrocytes to TBI……. 9

1.7 Schwann Cell Response to Traumatic Injury…… 10

1.7.1 Schwann Cell Description……... 11

1.7.2 Wallerian Degeneration of Schwann Cells……. 11

1.7.3 Signaling Response of Traumatic Injured Schwann Cells……. 12

1.8 Research Aims…….. 13

TABLE OF CONTENTS
(Continued)

Chapter **Page**

2 METHODS …… 15

2.1 Stretch Device……... 15

2.1.1 Culture Well……...……. 17

2.2 Cell Culture…….…….. 17

2.2.1 Coating……..……..... 17

2.2.2 Dorsal Root Ganglia Plating……..... 18

2.2.3 Schwann Cell Plating and Differentiation…… 18

2.2.4 Media…….. 18

2.3 Characterization……...……. 19

2.3.1 Stretch Response of Axon……..…… 19

2.3.2 Fluorescence Microscopy and Analysis……. 20

2.3.3 Microscopy……. 21

3 RESULTS ……..…… 22

3.1 Axon Response to Stretch Injury……..…….……...… 22

3.1.1 Axon Morphology Response to Stretch Injury……..……..... 22

3.1.2 Quantitative Outline of Axonal Response to Injury……... 25

3.1.3 Calcium Response to Axon Stretch Injury…...…….. 26

3.1.4 Changes in Axon Structure After Stretch Injury...…….. 30

3.2 Schwann Cell Response to Stretch Injury.……...… 30

3.2.1 Calcium Response in Injured Undifferentiated Schwann Cells…….. 30

TABLE OF CONTENTS
(Continued)

Chapter	Page
3.2.2 Calcium Response in Uninjured Undifferentiated Schwann Cells…….	34
3.2.3 Calcium Response in Differentiated Schwann Cells……..	36
4 DISCUSSION.....……..……...	40
4.1 DRG Approach to Stretch Injury…….…….	40
4.2 DRG Pathology Induced by Stretch Injury..…….	40
4.2.1 Axonal Parameters for Stretch Injury…….	42
4.2.2 Axonal Delayed Response to Stretch Injury……...	43
4.2.3 Axonal Degenerative Response to Stretch Injury……..	44
4.3 Calcium Response in Stretch Injured Axons…...…….	45
4.3.1 Two Phases of Calcium Increase……	45
4.3.2 Both Phases of Calcium Influx Depend on Extracellular Calcium…….	47
4.3.3 Mechanism of Calcium Pathology Underlying Axon Stretch Injury……..	47
4.4 Calcium Response in Stretch Injured Schwann Cells……...	50
4.4.1 Undifferentiated Schwann Cells Response to Stretch Injury….…….	50
4.4.2 Differentiated Schwann Cells Response to Stretch Injury……..	51
4.4.3 Additional Pathway for Intracellular Calcium Increase……..	52
5 CONCLUSIONS..…….…….	54
5.1 Coculture Signaling Between Axons and Schwann Cells…...……..	54
5.2 Coculture Signaling Between Axons and Oligodendrocytes…….	54
5.3 Similar Signaling Mechanism of Myelinating Glial Cells……..……...	55

TABLE OF CONTENTS
(Continued)

Chapter	**Page**
5.4 Final Statements.....……....	56
REFERENCES ……...	58

CHAPTER 1

INTRODUCTION

1.1 Brain Trauma

Brain trauma or traumatic brain injury (TBI) is a consequence from a serious head injury causing intrastructural-altering damage. While TBI is a major cause of death and disability in children and adults worldwide, pervasive neurological disorders are the more common outcome (Blumbergs et al., 1989; Smith et al., 1999; Ghajar, 2000; Maas et al., 2008). People whom suffer TBI can result with either complete recovery, permanent disability such as motor or cognitive dysfunction, or death (Teasdale and Jennett, 1974; Wilson et al., 1998). The level of brain impairment and whether it will be temporary or permanent is dependent on the extent of damage (Teasdale and Jennett, 1974; Blumbergs et al., 1989; Wilson et al., 1998; Gennarelli et al., 1998).

Brain trauma can result either with or without external contact. Without external contact abrupt acceleration or deceleration causes TBI. In a severe occurrence, such as car accidents, the head is inadvertently altered rapidly from its current position. External contact or blunt trauma to the head, seen in sports induced concussions, can cause damage (Adams et al., 1982; Adams et al., 1992; Graham, 1996; Bramlett and Dietrich, 2004). TBI can cause visible damage seen as skull fractures or unobservable brain damage at the cellular or subcellular level (Graham, 1996; Bramlett and Dietrich, 2004). The characteristics and severity of TBI are determined by intensity, direction and contact of the forces exerted. Forces applied in TBI are classified by their direction along an axis and/or movement around a fixed axis (Holboum, 1943; Maxwell, 1996). The external

forces cause deformation to the cerebral tissues of the brain (Holboum, 1943; Adams et al., 1992; Graham, 1996). This deformation of the brain microscopically distorts the structures of the neurons, the signaling cells of the central nervous system (CNS).

1.2 Diffuse Axonal Injury

The common pathology following TBI can be described as focal (located to a specific area), or diffuse (broadly distributed) (Gennerali et al., 1982). Diffuse axonal injury (DAI) is defined as the widespread damage, which is localized in some areas, to individual neurons and loss of connections between their axons in the grey and white matter of the brain (Strich, 1961; Peerless and Rewcastle, 1967; Blumbergs et al., 1989). Further observation of DAI determined that lesions in the white matter tracts are more common than in grey matter (Strich, 1961; Zimmerman et al., 1978; Adams et al., 1982; Blumbergs et al., 1989).

DAI pathology following injury results with the tissue in the white matter forming lesions and then the immediate disconnection of axonal connections (Maxwell et al., 1993; Povlishock and Christman, 1995). The term primary axotomy was described as the rapid degradation and subsequent disconnection of the axons occurring within minutes of injury (Maxwell et al., 1993). This included the fragmentation of the axolemma (axon membrane) and the appearance of a shredded or torn terminal end (Maxwell et al., 1993). This type of injury occurs when axons are exposed to high levels of tensile strain (Holboum, 1943; Margulies et al., 1990; Maxwell et al., 1993).

Secondary axotomy in DAI is the delayed disconnection of axonal connections (Povlishock et al., 1992; Maxwell et al., 1993; Smith et al., 1999; Gaetz, 2004). Studies

have identified no fragmentation but perturbation to the axonemma causing pathological intracellular signaling cascades, focal impairment of axonal transport (the anterograde and retrograde transport of cargo such as organelles and proteins) and the accumulation of the discharged cargo and cytoskeletal components, which is viewed by microscopy as swellings along the axon, preceding the delayed disconnection of the axonal body (Povlishock et al., 1992; Maxwell et al., 1993; Maxwell, 1996; Matute and Ransom, 2012). Investigation over extended time periods concluded secondary axotomy can occur hours to days following injury (Gennarelli et al., 1982; Povlishock et al., 1992; Maxwell et al., 1993; Gaetz, 2004).

DAI induces varying degrees of tissue damage in the white matter (Povlishock et al., 1992; Wolf et al., 2001). The more common outcome of DAI is secondary axotomy where the axons remain attached after applied forces but gradually become dysfunctional and degenerate over time (Maxwell et al., 1993). This type of axonal injury is further being investigated for interventional targets in the progressive detrimental pathology.

1.3 Myelinated Axon Response to DAI *In Vivo*

1.3.1 Axon Response to DAI

Studies have looked at cerebral tissue in patients with severe post traumatic dementia to study the effects of DAI and identify structural changes to the white matter tracts (Strich, 1961; Blumbergs et al., 1989). A research model using primates applied angular acceleration to the head and showed similar axonal damage as seen in humans with DAI (Gennerali et al., 1982; Gennerali et al., 1985; Blumbergs et al., 1989). Another study was developed using rats, applied impact acceleration by a combined linear and angular

head impact, mimicking a closed head injury and caused significant axonal injury in white matter fibers (Marmarou et al., 1994).

Successive to a traumatic event, axonal injury in DAI is associated with diffuse damage; evident by axonal swellings or retraction balls and localized in various white matter tracts (Blumbergs et al., 1989; Maxwell et al., 1993). A study revealed TBI induced axon injury within the optic nerve of mice produced the pathobiology associated with axon injury by the apparent axonal swellings and disconnections (Wang et al., 2011).

Antibodies have been used to determine degenerative axon biopathology by targeting intracellular or extracellular proteins associated with the cell structure or signaling molecules. The pathogenesis of traumatically induced axonal damage in secondary axotomy shows the accumulation of organelles and cytoskeletal components, both of which express specific protein markers making them identifiable and traceable by immunocytochemistry (Povlishock et al., 1983; Yaghmai and Povlishock, 1992; Maxwell et al., 1993; Smith et al., 1999; Li et al., 2011). Studies have identified the disruption to the axonal cytoskeletal and disconnection of its component by antibody treatment recognizing β-amyloid precursor protein (β-APP) (Yaghmai and Povlishock, 1992; Stone et al., 2004; Wang et al., 2011).

1.3.2 Myelin Response to DAI

Axons in the white matter of the central nervous system are cortical neurons which have insulating sheaths of myelin around their axons. The loss or lack of myelin will cause dysfunction or failure of the neurons and the nerves progressively degenerate (Stankoff et al., 2006). A major clinical issue is to assess and quantify myelin *in vivo* (Wang et al.,

2009). MRI is one method used for diagnosing and monitoring white matter diseases (Barkovich, 2005). Unfortunately diffuse injury has more microscopic injury than macroscopic injury and is difficult to detect with MRI (He et al., 2005; Wang et al., 2009). Magnetization transfer (MT) and diffusion tensor imaging are used to assess pathological mechanisms involved in human white matter damage. The decrease in thickness of a white matter axon, using an MT, indicates a loss of myelin but also axonal degeneration (Fillipin et al., 2005; Stankoff et al., 2006). Diffusion weighted imaging (DW-MRI) differentiates tissue microstructure and white matter tracts in the brain but not between myelin and axon injury (Le Bihan et al., 2001).

1.4 DAI *In Vitro*

DAI *in vitro* studies focus on the molecular and cellular mechanisms underlying cell dysfunction and death (Graham, 1996; Smith et al., 1999; Wolf et al., 2001; Bramlett and Dietrich, 2004). DAI research has used an *in vitro* dynamic stretch injury device, which was conducted on non-myelinated cortical axons, to cause and further evaluate axonal damage (Smith et al., 1999). The morphologic characteristics following stretch injury of the cortical axons and mechanical loading conditions were assessed; the axonal damage resulted in axonal swellings similar to the biopathology of humans suffering brain trauma.

1.4.1 *In Vitro* Injury Model

DAI *in vitro* studies have modeled the molecular biopathology similar to axonal injury in humans by using devices which mimic the mechanical loading of the intracranial environment occurring during TBI. TBI results in the axons to be microscopically

stretched longitudinally or uniaxially (Adams et al., 1992; Graham, 1996; Bramlett and Dietrich, 2004). The uniaxial stretch causes intermittent structural damage to the axonal body (Blumbergs et al., 1989). Some injury models are designed to cause uniaxial stretching of axons. A stretch injury model mechanically applied uniaxial stretch to axons at specific strains (Smith et al., 1999). Using this device, the axonal damage after injury was continuously observed and characterized.

The stretch injury model, from Smith's lab at the University of Pennsylvania, consists of culturing cells on a thin elastic silicone membrane. The inversed application of pressure to the pliable membrane causes it to deform downward. Placing the culture on a rigid plate, with a rectangular slit along the center alignment, isolated the stretch injury. The pressure applied to an isolated area of cortical axons, grown perpendicularly across the injury site, causes uniaxial stretching of the axons.

$$\dot{\varepsilon} = \frac{d\varepsilon}{dt} = \frac{d}{dt}\left(\frac{l - lo}{lo}\right) \tag{1.1}$$

The extent of stretch or elongation of the axons is manipulated by the applied strain (ε), the amount of deformation or change in length $(l - l_o)$ with respect to the original length (l_o). The amount of damage to the axon is also dependent on the strain rate $(\dot{\varepsilon})$, the rate of change in strain with respect to time.

1.5 *In Vitro* Stretch Injury Model

This *in vitro* research of white matter has been implemented on un-myelinated cortical neurons (Smith et al., 1999). The physiology of axonal swellings randomly distributed

along the length of the axon, neurofilament accumulation, primary axotomy, calcium influx and axonemma channels were analyzed after injury by the uniaxial stretch injury device (Smith et al., 1999; Wolf et al., 2001).

1.5.1 Axonal Response to Stretch Injury Model

Axonal physiology of cortical neurons, such as distortions or undulations along the axon, was demonstrated after applying strains using the *in vitro* stretch injury model (Smith et al., 1999). The reorganization of the cytoskeleton was visualized by the recovery of the axons to their preinjured orientation.

The intra-structural damage from DAI is microscopically viewed externally as axonal swellings which arbitrarily occur along the axon (Gaetz, 2004; Kilinc et al., 2008). This is caused by the accumulation of proteins and organelle cargos, due to a compromised axonal transport system (Maxwell, 1996). Axonal transport is the transportation of cargo to and from the cell body along the axon on an intracellular cytoskeleton structure. The neuronal proteins are transcribed in the cell body and vital for the neurons functionality and survival. The axonal swellings were apparent after *in vitro* stretch injury to un-myelinated cortical axons and had accretion of neurofilament proteins (component of cytoskeleton structure) (Smith et al., 1999). Fast axonal transport along microtubules, a supra-cytoskeleton intracellular structure, was analyzed to deduce the localization of transport restricted proteins in the axonal swellings (Smith et al., 1999; Tang et al., 2010).

An axon which appears to be stable following injury, characterized at the molecular level, indicates detrimental signaling cascades which could underlie the pathology for delayed fragmenting and disconnection of the axon (Raff et al., 2002;

Lingor et al., 2012). These cascades are postulated to be initiated by a pathologic rise in intracellular calcium (Weber, 2012). Wolf's study, using the *in vitro* stretch injury model, demonstrated an influx of calcium after stretch injury to axons and indicated a primary role of tetrodotoxin (TTX) sensitive voltage gated sodium channels, ω-conotoxin MVIIC (CTX) sensitive voltage gated calcium channels, and bepridil (Bep) sensitive sodium-calcium exchanger (Wolf et al., 2001). The inhibition of these channels decreased the rise in intracellular calcium concentration after injury and identified the role of each in the calcium influx into the cell.

1.5.2 Myelinated Axon Response to Stretch Injury Model

To further study the effects of DAI on white matter, the biopathological changes of myelin would be evaluated using the stretch injury model on myelinated cortical axons. The *in vitro* limitation for white matter injury is that cortical neuron cultures have not been able to remain healthy long enough to support oligodendrocytes, central nervous system (CNS) myelinating glial cells, to myelinate axonal extensions.

1.6 Myelinated Axon Studies

Myelinated axons are neurons which have insulating sheaths of myelin wrapped around their extensions. Myelin acts as an electrically insulating material which enables action potentials (membrane potential spikes) to travel faster along the axon. The cytoplasm of an axon is electrically conductive and the encompassing myelin inhibits charge leakage through the membrane (Barrett et al., 1982). The myelin sheath runs along the axon in sections which are divided by unsheathed nodes of Ranvier. The nodes contain a high density of voltage gated ionic channels (Salzer, 1997). An increase in voltage at one

node of Ranvier will extend spatially to the next node and is great enough to elevate the voltage at that node; mechanistically referred to as saltatory conduction (Huxley and Stampfli, 1949; Barrett et al., 1982). Thus in myelinated axons action potentials recur at successive nodes and hop along the axon faster than unmyelinated fibers where impulses move slower and continuously (Hartline and Colman, 2007).

The significance of myelin loss after TBI is associated with neurological dysfunction (Stankoff et al., 2006). The damage to the myelin and axon impairs the conduction of signals in the affected nerve and cell-cell communication. This is the basis for a TBI patient to be deficient in sensation, movement, cognition, or other functions depending on which nerves are involved (Bramlett and Dietrich, 2004).

The myelin sheath is wrapped around the axon by the extending processes from oligodendrocytes, myelinating CNS glial cells. One oligodendrocyte provides support and insulates multiple axons.

1.6.1 Oligodendrocytes Response to TBI

The fate of viable oligodendrocytes after TBI is unclear. Studies have shown demyelination at the injury site was amongst apoptotic cells which were positive for oligodendrocyte markers (Crowe et al., 1997). The demyelination and apoptotic cells were also present distally from the injury site and suggested the demyelination of CNS white matter could be due to active cell apoptosis or passive necrosis. The axons of secondary axotomy may fail to support oligodendrocyte survival resulting in the observed apoptosis of these cells (Shuman et al., 1997). If these axons can support oligodendrocyte remyelination, which has been shown to spontaneously occur in the healthy CNS, is also questioned (Bunge et al., 1961).

1.6.2 Calcium Response in Oligodendrocytes to TBI

A compromising stimulus, whether mechanical or chemical, has been shown to influence intracellular calcium signals in myelinating cells (Verkhratsky et al., 1998). For instance, electrical stimulus by oscillations to the optic nerve causes correlating oscillations in the intracellular calcium level of oligodendrocytes (Kriegler and Chiu, 1993). Excitotoxicity, the excessive release of a neurotransmitter and the over stimulation of amino acid receptors, plays a major role in the secondary injury and death of cells (Weber, 2012). High levels of intracellular calcium are sustained by a toxic influx of extracellular calcium entering the cells through calcium permeable ion channels. Sustained high levels of intracellular calcium are responsible for cell damage and death (Weber, 2012). Glutamate, a major excitatory neurotransmitter in the nervous system, activates the receptors on calcium permeable ion channels allowing the increased intracellular calcium concentration in glial cells (Matute and Ransom, 2012).

The intracellular calcium stores homeostasis are also crucial for a cells livelihood. The endoplasmic reticulum (ER) contributes to calcium exchange between its calcium store and the cytosolic levels of the cell. Severe or prolonged stress to the ER can induce apoptosis by activating caspase-12 (cell death initiator) during abnormal calcium influx (Nakagawa et al., 2000). The ER stress and excitotoxicity cause for intracellular calcium concentration to be increased has been inadvertently shown to cause demyelination through consequential oligodendrocyte death (Ruiz et al., 2010). The calcium response of oligodendrocytes to injury and their livelihood is an important factor to consider when analyzing the effects of TBI.

1.7 Schwann Cell Response to Traumatic Injury

There is no research directly demonstrating if myelin degeneration in DAI is due to oligodendrocyte death. Oligodendrocytes have been shown to myelinate dorsal root ganglia (DRG), the peripheral nervous system (PNS) neuron, in coculture studies (Chan et al., 2004). Analyzing myelin degeneration by stretch injury to oligodendrocyte myelinated DRGs would also have to determine oligodendrocyte response to injury. The effect of injury on Schwann cells, the PNS myelinating glial cell, can predict what to expect from future studies examining oligodendrocyte injury response and the injury response of myelinated DRGs.

1.7.1 Schwann Cell Description

Schwann cell myelinated axons are analogous to myelinating oligodendrocytes by which the gaps between the myelin segments are called the nodes of Ranvier and action potentials travelling distally along the axons are by saltatory conduction. Dissimilarly, myelinating Schwann cells wrap themselves around an axon with many revolutions (Geren and Schmitt, 1954). Each revolution or layer forms myelin in between and the covering they form over the axon is referred to as the myelin sheath. One Schwann cell is a myelin or myelin sheath segment of the myelinated insulators along the length of the axon. The process of the Schwann cell wrapping around the axon is referred to as myelination and was described as first, the Schwann cell making contact with the axon, the structural extension of the Schwann cell, axon ensheathment and finally myelin maturation by the Schwann cells continuous revolutions around the axon (layering) (Geren and Schmitt, 1954; Bunge et al., 1989).

1.7.2 Wallerian Degeneration of Schwann Cells

Primary or secondary axotomy of myelinated axons initiates a series of events distally from injury site. The distal stump undergoes Wallerian degeneration which is the degeneration of the myelin sheath, break down of the Schwann cells myelin and the viable Schwann cells will then dedifferentiate and proliferate (Scherer et al., 1996). A study demonstrated the addition of glial growth factor (GGF) to cultures, in which myelin had already been formed, resulted in demyelination associated with Schwann cell dedifferentiation and proliferation (Zanazzi et al., 2001). Demyelination was induced in a coculture of the Schwann cells on intact DRG axons. The demyelination was shown to be reversible, by the co-cultured Schwann cells remyelinating the bare axons. This study indicated the demyelination is specific, reversible, and a direct effect on the Schwann cells. Another research model showed the remyelination capability of Schwann cells on demyelinated axons by restoring the conduction velocity and ability to conduct trains of impulses by the axons (Felts and Smith, 1992).

1.7.3 Signaling Response of Traumatic Injured Schwann Cells

Demyelination in the peripheral nervous system has been postulated to be caused by a signaling pathway residing in myelin forming Schwann cells following traumatic injury. Injury has been shown to increase intracellular calcium in Schwann cells (Jahromi et al., 1992). The increased intracellular calcium after injury causes the delayed onset of cell damage and death (Ciutat et al., 1996). Activation of degradative enzymes such as proteases and endonucleases by the irregular intracellular calcium levels initiates signaling cascades which cause cell dysfunction and death (Trump and Berezesky, 1995). Some studies questioning this phenomenon have looked at possible neurotransmitter

initiators. Schwann cells were shown to release neurotransmitters aspartate and glutamate from a neuronal agonist signal (Parpura et al., 1995). Certain channels and associated neurotransmitters, such as the glutamate transporter and the glutamate neurotransmitter, have been hypothesized to be the components which alters intracellular calcium levels in glial cells (Choi and Chiu, 1997). Calcium overload to organelles, endoplasmic reticulum and mitochondria, can lead to functional failure and release of their calcium supply (Weber, 2012). The intracellular calcium concentration coupled with the calcium levels from damaged intracellular calcium stores and extracellular calcium entry collectively contribute to the high calcium concentration in the cell after injury.

1.8 Research Aims

The effect of stretch injury on non-myelinated DRG axons is determined by using a stretch injury device capable of viewing the injury to analyze the morphology and physiology at the time of injury and compare the sequential characteristics to what was seen *in vitro* in non-myelinated stretch injured cortical axons (Smith et al., 1999; Magou et al., 2011). The parameters for a mild injury were chosen based on the presence of beading and undulations arbitrarily occurring along the axon. Severe injury was defined by fragmentation and disconnection of the axon 24 hours after injury. The physiology of the axon was examined for a flux in intracellular calcium concentration by a mild and severe injury and the amount contributed by the extracellular calcium influx and the intracellular calcium stores release.

Analysis of Schwann cells was to determine the effect of stretch injury on their intracellular calcium levels. The calcium influx of the peripheral nervous system myelinating cell could predict what to expect from an oligodendrocyte injury. The difference in injury severity (severe and mild) was analyzed on undifferentiated (non-myelinating) and compared to differentiated (myelinating) Schwann cells.

There is no medical treatment for the progressive dysfunction and demyelination of the white matter fibers following TBI. Research has focused on the detrimental intracellular pathological mechanisms following traumatic injury for possible pharmaceutical intervention. These experiments demonstrate a way to evaluate possible treatments for the progressive biopathology and identify target proteins utilizing the stretch injury device.

CHAPTER 2

METHODS

2.1 Stretch Device

The stretch device consisted of an aluminum pressure chamber, a deformation mask with 2.0 mm slit, and an air pulse-generating system (Magou et al., 2011). The well insert consists of cultured cells on a thin elastic silicone membrane. The application of pressure to the membrane causes it to deform downward. Placing a mask below the membrane with a rectangular slit (approximately 2 mm x 18 mm) allows for a defined area to be displaced and microscopically viewed from below through the translucent membrane by a Nikon inverted microscope (Optical Apparatus, Ardmore, PA). In terms of neuronal cultures, dorsal root ganglia (DRG) neurons are plated on one side of the well and the axonal extension are grown across the center. The pressure applied leads to uniaxial stretching of the axon correlating to the deformation of the membrane which they are adhered to. Injured Schwann cell cultures are plated homogenously on the membrane. Refer to Figure 3.1 for well insert, deformation mask and chamber construct.

The injury system described previously by Magou et al., consisted of four components, a control system interpreted by LabVIEW (National Instruments, Austin, Texas), pressure regulator system, a valve control system, and a pressure sensor regulated injury chamber. The input pressure is supplied by a compressor air tank into a secondary supplier which is regulated by an electronic pressure controller with a mechanical blow-off valve (VSO-EP, Parker Hannifin, Life Sciences, Hollis, NH). The control system signals the valve driver circuit (OEM, Parker Hannifin) controls the valve, a three-way

normally closed fast-acting solenoid valve (Parker Hannfin, Life Sciences, Hollis, NH), connecting the secondary reserve tank to the injury chamber to deliver a controlled pressure pulse to the cultures.

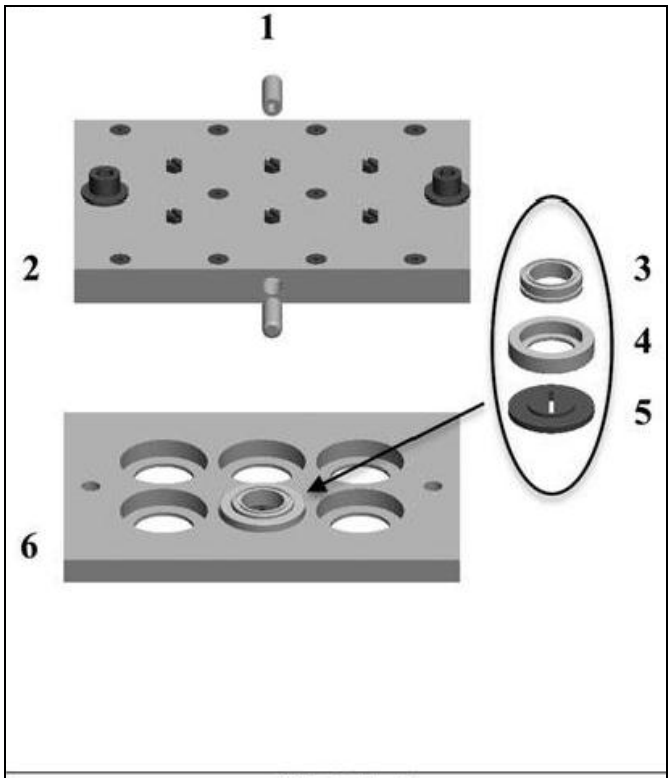

Module A (6-well)	
1	Pressure Inlet
2	Pressure Chamber (Top Plate)
3	6-well Vessel (Top Ring)
4	6-well Vessel (Bottom Ring)
5	Deformation Mask
6	Pressure Chamber (Bottom Plate)

Figure 2.1 6-Well Pressure Chamber with Removable Wells and Deformation Mask.

Source: GC Magou *et al.*, 2011.

2.1.1 Culture Well

This method is a modified version previously described by Magou et al., 2011. Injury wells are built by two composites made of polyether ether ketone (PEEK). The PEEK rings are sonicated for 30 minutes in 70% ethanol, wiped down by lint free Kimwipes, heated in boiling distilled water for 30 minutes and dried on Kimwipes. The silicone membrane (0.005“ gloss/gloss silicone sheeting, Specialty Manufacturing, Saginaw, MI) is cut into approximately 1.5 x 1.5 cm squares. A square of silicone membrane is sequestered between two peek rings, one smaller and fits into the larger ring (Figure 2.1). The smaller of the PEEK rings is secured by the encirclement of an O-ring fitting into a structural groove along the anterior wall. Completed wells are submerged in reverse osmosis (RO) water and autoclaved for 1 hour.

2.2 Cell Culture

2.2.1 Coating

After autoclaving, all PEEK tissue culture plates and wells were allowed to dry and cool to room temperature in a sterile tissue culture hood. Silicone substrates were then coated with poly-d-lysine (10 µg/mL, PDL, BD, Bedford, MA) for 1 hour. PDL solution was aspirated and wells were rinsed. They were then coated with 250 µL of matrigel each (Figure 2.1) (250 µg/mL, Growth Factor Reduced (GFR) Matrigel Matrix, Bedford, MA). This was determined to be the least amount of volume for full equated coverage of surface. Coated wells were left uncovered to dry. Wells were then rinsed with Dulbecco's modified eagle medium (DMEM) and left to completely dry before plating.

Figure 2.2 Homogeneous matrigel coated culture well.

2.2.2 Dorsal Root Ganglia Plating

Dorsal root ganglia (DRGs) were isolated from gestational day 16 (E16) rat embryos, dissociated in 0.25% Trypsin (Invitrogen, Carlsbad, CA) for 35 minutes. After dissociation, neurons were plated at an average density of seven dissociated embryonic DRG explant/well. A 75 µL droplet was plated on the edge of the vessel. Cells were allowed to adhere to substrate for three hours followed by addition of 600 µL DRG media with forskolin (10 µg/µL, Forskolin, Sigma). Media was changed every two days with DRG media for 12 days.

2.2.3 Schwann Cell Plating and Differentiation

Primary Schwann cells (SCs) were cultured as described (Brockes et al., 1979). Cells were passaged upon confluence and used at 3-7 passages. Schwann cells were plated at an average density of 400,000 cells/well. Schwann cell differentiation was induced with 750 uM dbcAMP (dibutyryl cyclic AMP, dbcAMP, Sigma) for 48 hours after having been plated for at least 24 hours.

2.2.4 Media

DRG Media formulation: Neurobasal (Invitrogen) supplemented with B-27 (Invitrogen), penicillin/streptomycin (Invitrogen), and 200 mM of L-Glutamine (Invitrogen). SC

Media: DMEM supplemented with 10% heat inactivated fetal bovine serum (FBS) (HyClone, Logan, UT), penicillin/streptomycin (0.1 mg/ml) and glutamax supplement (Invitrogen). SC Differentiation Media: DMEM supplemented with 2% heat inactivated fetal bovine serum (FBS) (HyClone, Logan, UT) and penicillin/ streptomycin (0.1 mg/ml), glutamax supplement (Invitrogen) and dbcAMP (0.1 mg/ml, dibutyryl cyclic AMP, dbcAMP, Sigma).

2.3 Characterization

2.3.1 Stretch Response of Axon

The gradual reorganization of the axonal body into its straight orientation was compared to its uninjured configuration and the variance was quantified. A time-lapse phase contrast sequence was collected for a one hour period. An initial image was taken at various locations within the injury area. The sequence was taken at one of these points immediately after injury; the one chosen was based on microphotographic integrity of the view plain. Recordings were collected every 30 seconds for 1 hour. The sequence was transferred from its collected stacks to images using an image analysis program (ImageJ, West Chester, PA). The program was then used to measure the length of the axon before and 0, 10, 20, 30, 40, 50 and 60 minutes after injury. The axon was identified by morphologic markers, abridgement by another axon and/or debris in view. The view plain was chosen based on the capability to identify and substantiate a defined region was being measured. The data presented determined the true change in length for an undulated axonal body.

Morphological response over time was quantified and previously described (Smith et al. 1999). The measured length of the undulation following injury was compared to the measurement of the uninjured axonal extension. This value is defined as $D(t_i)$ and determined by the gradual variance in measured length of the axon sequentially after injury $L(t_i)$ compared to the axonal regional length before stretch L_o:

$$D(t_i) = L(t_i)/L_o \quad (2.1)$$

The before stretch value would be 1.0, comparing the length of it to itself. The $D(t_i)$ quantification after injury, having an increase in length from being stretch and not retracting itself immediately after with a delayed elasticity seen as an adhered distorted axon, will be above 1.0 in each analyzed trial.

2.3.2 Fluorescence Microscopy and Analysis

Fluor-4 staining as described (Smith et al., 1999). Briefly, cells were loaded with 2 µM fluo-4 AM ester (Molecular Probes, Eugene, OR) solubilized in dimethylsulfoxide (DMSO) (0.05% final) with pluronic F-127 [0.004% (w/v) final] in Hank's balanced salt solution (HBSS, Calcium, Magnesium, no Phenol Red, Invitrogen). The dye solution was loaded for 30 min; the solvent was aspirated and the cell were loaded with HBSS for 30 min and then rinsed twice before injury. Injury was induced with calcium present extracellularly. For the control experiment analyzing DRG calcium influx at the time of injury to be extracellularly supplied and to what degree, the dye solution was loaded for

30 min; the solvent was aspirated and the cell were loaded with HBSS without calcium and magnesium for 30 min, and then rinsed twice before injury.

Fluorescence microscopy was performed on a Nikon TE2000-S inverted microscope. The dye was illuminated at 488 nm and collected at 515 nm by the emitted fluorescence. Fluorescence images were collected and analyzed using time-lapse software (Q-Imaging; Q-Capture Pro, Surrey, B.C., CA) to create time-lapse sequences. DRG experiment; images were taken at 30 msec intervals for 5 minutes, followed by 30 sec intervals for 55 minutes. The injury was induced approximately 8 seconds after initial image was taken. Schwann cell experimental images were taken at 30 msec intervals for 3 minutes.

Analysis of fluorescence with fluo-4 dye was performed on ten representative axons from each culture. Axons were excluded from analysis if they had structural damage from loading. Arbitrary regions from each axon were analyzed and then averaged. Quantifying the fluorescence for each axon was executed by self-ratios of the measured fluorescence sequential to injury (*F*) and the fluorescence of an uninjured axon (*Fo*). Background noise was abolished by continuously sampling three voided areas. The mean of these values was subtracted from the measured fluorescence (*F*). The same principles were used for Schwann cell experiments, 20 cells were analyzed per well, 10 neighboring cells in two locations of the well were chosen indiscriminately.

2.3.3 Microscopy

Phase-contrast imaging and fluorescent photomicrography were performed on a Nikon TE2000-S inverted microscope. Sequential images were collected by a 0.63x camera lens using time-lapse software (Q-Imaging; Q-Capture Pro, Surrey, B.C., CA).

CHAPTER 3

RESULTS

Mimicking the biopathology of brain trauma on cultures using an *in vitro* stretch injury model, capable of real time imaging, allows for the analysis of morphological and physiological traits immediately and continuously after injury. The device is able to control the severity of injury by the adjustable parameters, strain and strain rate, applied to the cultures.

3.1 Axon Response to Stretch Injury

3.1.1 Axon Morphology Response to Stretch Injury

Stretch injured axons remained adhered to the membrane but showed undulations randomly occurring along the length of the axon immediately and continuously after injury. Undulations were evident at all biomechanical parameters used in the experiments (60% and 90% strain; 30 s^{-1} strain rate). The occurrence of undulations along the axon body was not dependent on the severity of injury. The axons demonstrated an active change in structure by gradually recovering to their preinjured orientation. This was evident to occur within one hour after injury. A delay in recovery was apparent for a severe injury, the maximum strain parameter analyzed, holding its disfigurement 20 minutes after injury when the structure began to actively reorganize (Figure 3.2). The milder applied strain showed recovery within the first 10 minutes of injury (Figure 3.1). The experimental analysis of active undulations after stretch injury was apparent in multiple trials. A severe injury showed fragmentation and axonal

thinning 24 hours after injury (Figure 3.2). The milder strain parameter showed structural integrity and no fragmentation after the same time period (not shown).

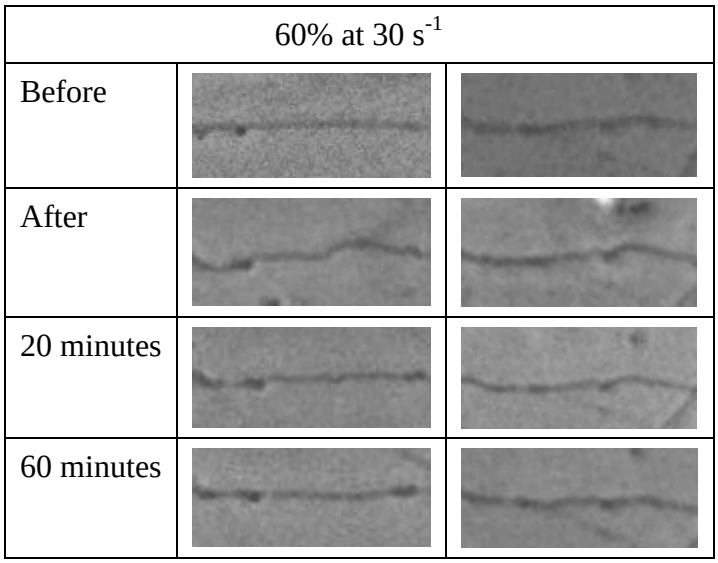

Figure 3.1 Two examples of the delayed response of axons to stretch injury at 60% strain 30 s^{-1} strain rate. Restructuring of the axon body is observed after injury by the preceding morphology from a straight orientation to random undulations along the axon, caused by mechanical loaded stretch injury, followed by active recovery to the original length within 1 hour.

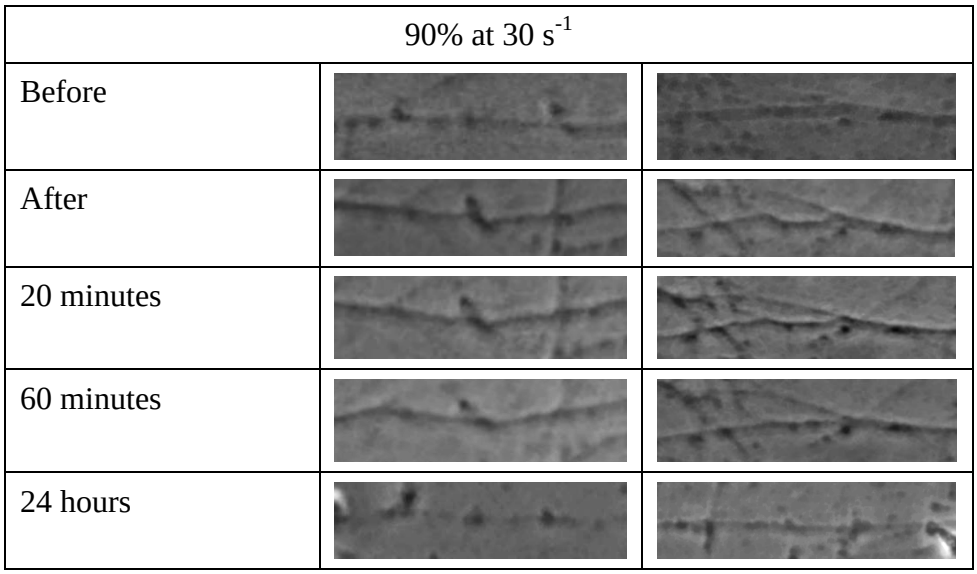

Figure 3.2 Two examples of the axonal body's delayed response to stretch injury at 90% strain 30 s^{-1} strain rate. Restructuring of the axon body from the previous morphology, before injury, of a straight orientation to randomly distributed undulations, followed by active recovery to the original length within 1 hour. The axon showed thinning and fragmentation evident in its structure 24 hours post injury.

3.1.2 Quantitative Outline of Axonal Response to Injury

The gradual recovery of an undulation in an injured axon can be quantified by the measurable geometric change after stretch using the time-lapse images. The analysis was confined to one of the undulations in an axon. The region of interest was deduced by morphological markers or imperfections, such as the traversing of another axon or beading, which allowed the tracking of an undulation. The stretch caused a 7-8% increase in length for both the severe and mild injuries, analyzed immediately after retraction of the deformed membrane (Figure 3.3). This indicated the displacement of a undulation was not dependent on severity. The severe injury showed a delay in retraction for the first 20 minutes whereas a mild injury showed recovery within the first 10 minutes. The attenuation of decrease in length was approximately 50 minutes after both injuries. The occurrence of the undulations varied between each axon. Overall, the comparison between the two severities shows the displacement of each undulation is not a significant factor but their kinetics sequential to injury is.

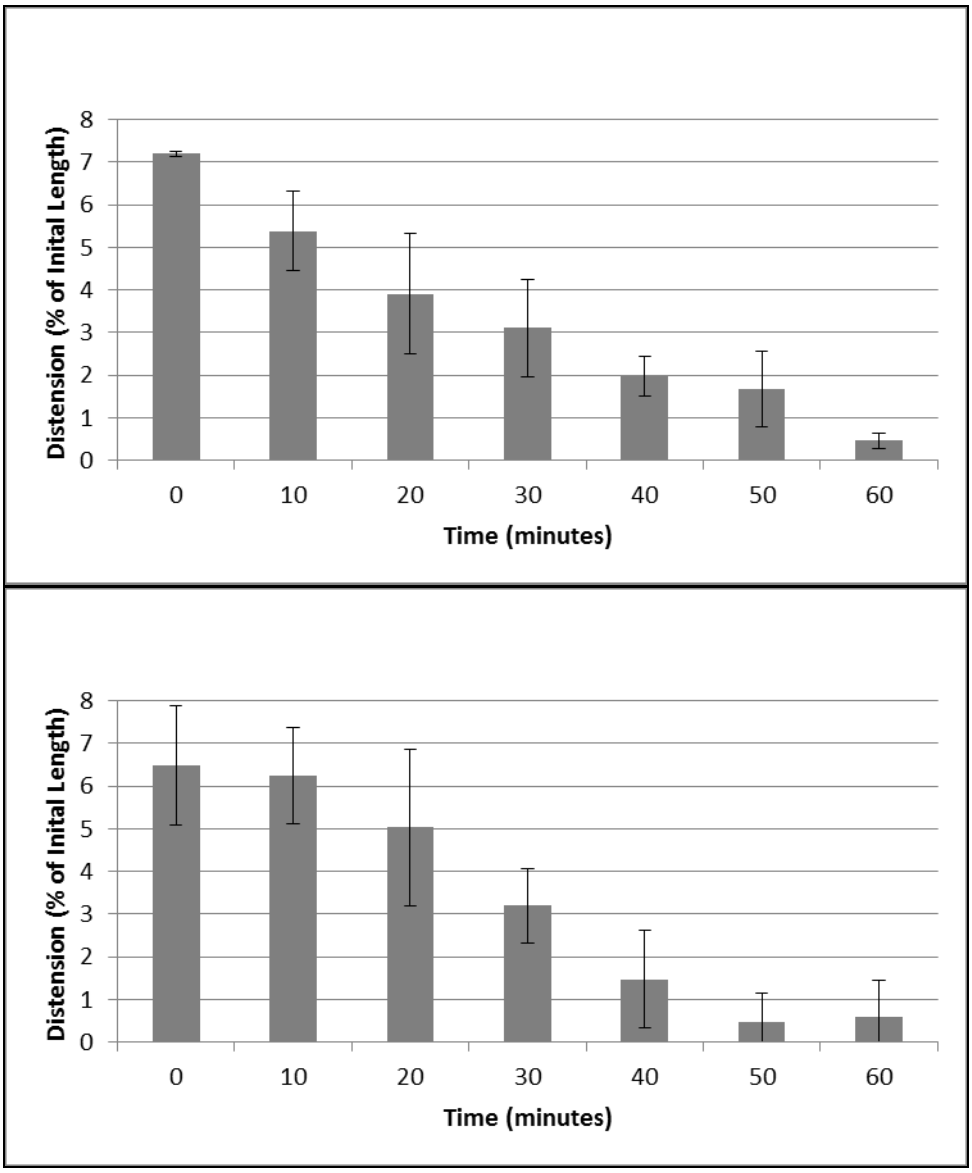

Figure 3.3 Quantitative representation of axonal response to stretch injury. *Top,* 60% strain at 30 s^{-1} strain rate. The average percent change in length of 12 undulated axon regions over a 1 hour period from the time of injury. *Bottom,* 90% strain at 30 s^{-1} strain rate, the average percent change in length of 12 undulated axon regions over a 1 hour period from the time of injury.

3.1.3 Calcium Response to Axon Stretch Injury

In severe and mild injury, uninjured axons observed baseline fluorescence from the fluo-4 calcium indicator stain, indicating the absence of overexposure in the following experiments. There was a minor variation in brightness for the analyzed axons in each

experiment but not significant to indicate a debatable analysis. In a severe and mild injury, without primary axotomy, there was a large increase in the fluorescence intensity at the time of injury (Severe, *F/Fo* = 4.77; Mild, *F/Fo* = 4.67) (Figure 3.4, 3.5). This correlated to the increase in intracellular calcium concentration. Subsequently, there was an immediate downward trend till the 20 second time point. There was consistency in the analyzed responses for the axons in each experiment, the increase in intercellular calcium concentration at the time of injury and decline over the 20 second time period (Figure 3.5). Exclusively to a severe injury, the fluorescence then underwent a significant consecutive increase for the following 60 minutes (Figure 3.5) (t = one minute, *F/Fo* = 1.96; t = 20 minutes, *F/Fo* = 11.35).

For axons injured in calcium-free HBSS ($[Ca^{2+}]_o$), immediately after injury there was a minor increase in the measured fluorescence correlating to the subtle increase in intracellular calcium (Table 3.1) (Severe, *F*/*Fo* = 1.75; Mild, *F/Fo* = 1.21). Conversely, there was no sequential increase in fluorescence for a severe injury in the absence of extracellular calcium after the immediate decline to baseline, correlating to no intercellular calcium increase following injury (t = 20 seconds, Severe, *F/Fo* = 1.32 and Mild, *F/Fo* = 1.22; t = 20 minutes, Severe, *F/Fo* = 1.20 and Mild, *F/Fo* = 0.80).

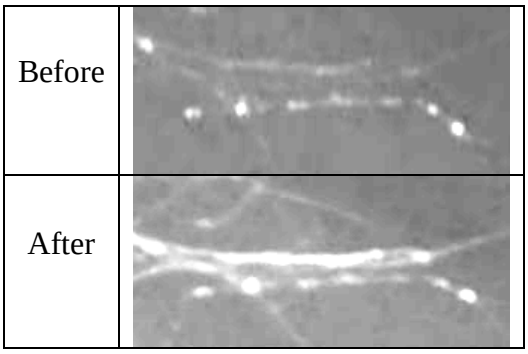

Figure 3.4 Fluorescence microscopy imaging of axons before and after injury indicating the calcium influx by change increase in fluorescence intensity.

Table 3.1 Measured Fluorescence Intensities of Calcium in Axons

	90%	60%	90% no $[Ca^{2+}]_o$	60% no $[Ca^{2+}]_o$
Before Injury	1	1	1	1
0 (At Injury)	2.775994	3.413197	1.746177	1.207683
0.005	4.775163	4.667935	1.599001	1.267802
0.01	4.803551	4.112483	1.672853	1.278733
0.05	4.016363	2.41977	1.536018	1.258088
0.2	2.03422	1.33354	1.323925	1.219226
1	1.96852	1.253037	1.27282	1.017613
3	4.373073	1.220588	1.100861	0.769246
5	6.648353	1.041537	1.006547	0.591921
10	9.736436	0.967713	0.926046	0.734537
20	11.35529	1.392374	1.209471	0.802414

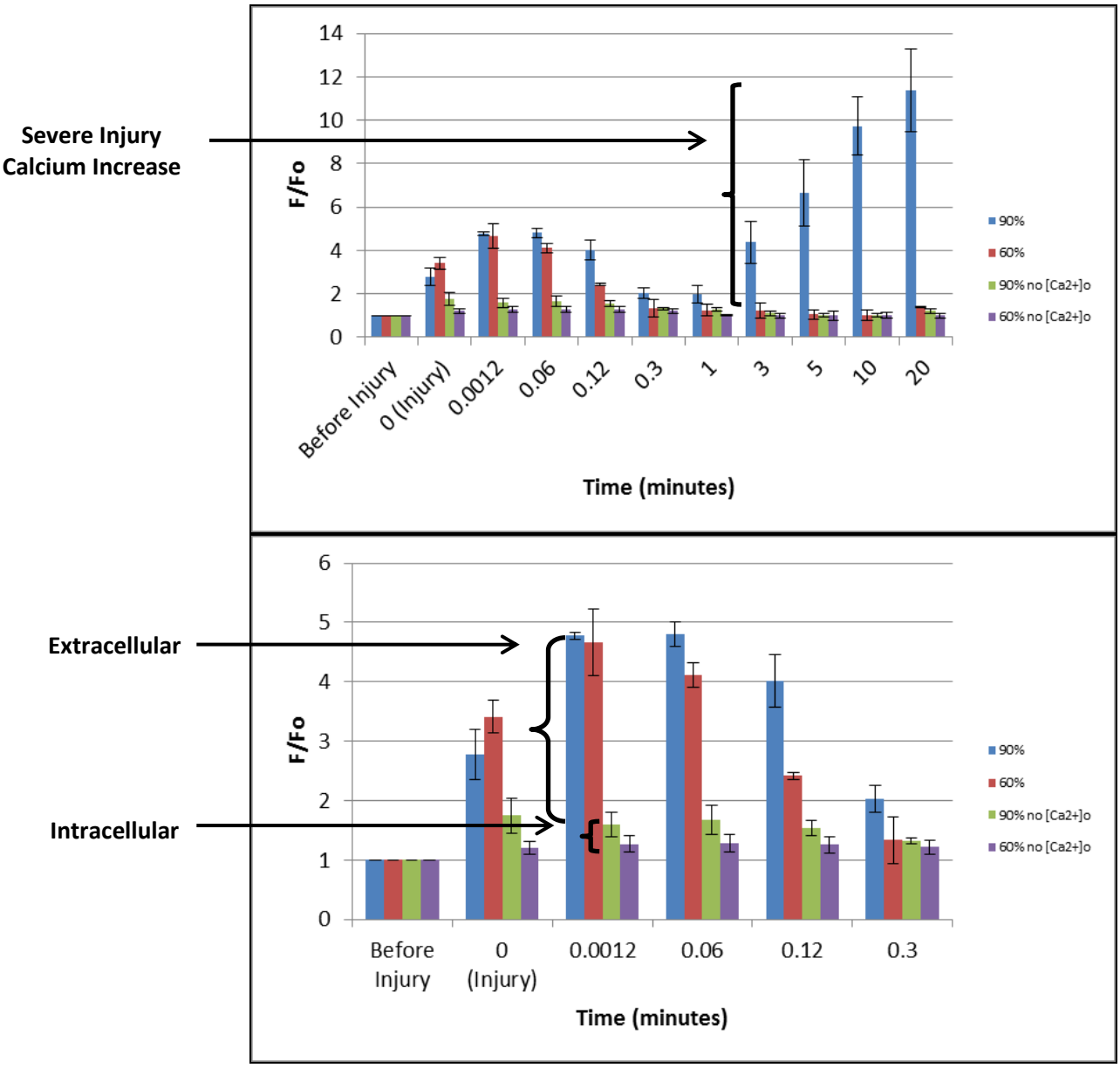

Figure 3.5 Successive change in calcium indicator fluorescence intensity immediately and continuously after stretch injury. *Top*, The change in fluorescence intensity over 20 minutes. *Bottom*, The same sequence for 20 second time period. Severe injury (90%, n = 27 axons), Mild injury (60%, n = 27 axons), calcium free serum ($[Ca^{2+}]_o$, n = 9 axons). *F*/*Fo* = change in calcium indicator fluorescence intensity over initial fluorescence.

3.1.4 Changes in Axon Structure After Stretch Injury

Multiple swellings along the length of the axon had a defined shape 30 minutes after stretch injury, observed by phase microscopy in both injury severities (Figure 3.6). Fluorescence microscopy, using calcium indicator stain (Fluo-4), revealed that the beadings were composed of accumulated calcium due to an increased areal volume randomly segmented along the axon following injury (Figure 3.6). The swellings were observed 60 minutes after injury by time-lapse imaging of the calcium fluorescence stained axons and phase microscopy. The beadings served as location markers for the verifying of a fragmented and thinned axon 24 hours following a severe injury (Figure 3.2).

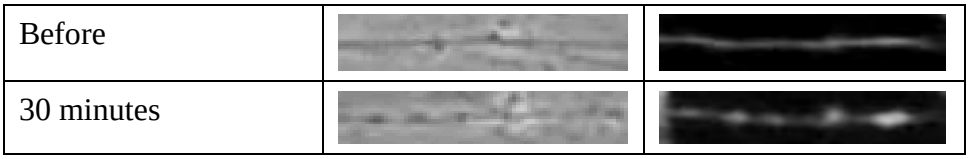

Figure 3.6 Axonal swellings after a mild stretch injury. *Left*, one example of axonal beading, microscopy image before and 30 minutes after injury. *Right*, one example of axonal beading, fluorescence images before and 30 minutes after injury.

3.2 Schwann Cell Response to Stretch Injury

3.2.1 Calcium Response in Injured Undifferentiated Schwann Cells

To test for over exposure of the fluorescence light the experiment was conducted with fluorescence observation and without injury. Baseline fluorescence was observed in non-injured Schwann cells, using the calcium indicator fluo-4 ($F/Fo \sim 1$), corresponding to no hindrance to the experimental integrity (Figure 3.8). The injured Schwann cells had a moderate increase in the measured fluorescence immediately after a mild injury and a

higher intensity in the severely injured cells (Severe, *F/Fo* = 3.4; Mild, *F/Fo* = 1.5) (Figure 3.7, 3.8). This indicates an injury induced rise in intracellular calcium concentration and a severe injury causing more calcium accumulation than in a mild injury. The severe injury, however, did not reach baseline fluorescence as soon as a mild injury. At approximately 2 minutes following injury the mild injured cells reach baseline (*F/Fo* ~ 1), whereas the severely injured cells were still approaching this level of fluoresce after 3 minutes (Figure 3.8). This indicates the ability of mild injured cells to have intracellular homeostasis and removal of excess intracellular calcium simpler and quicker than severely injured cells.

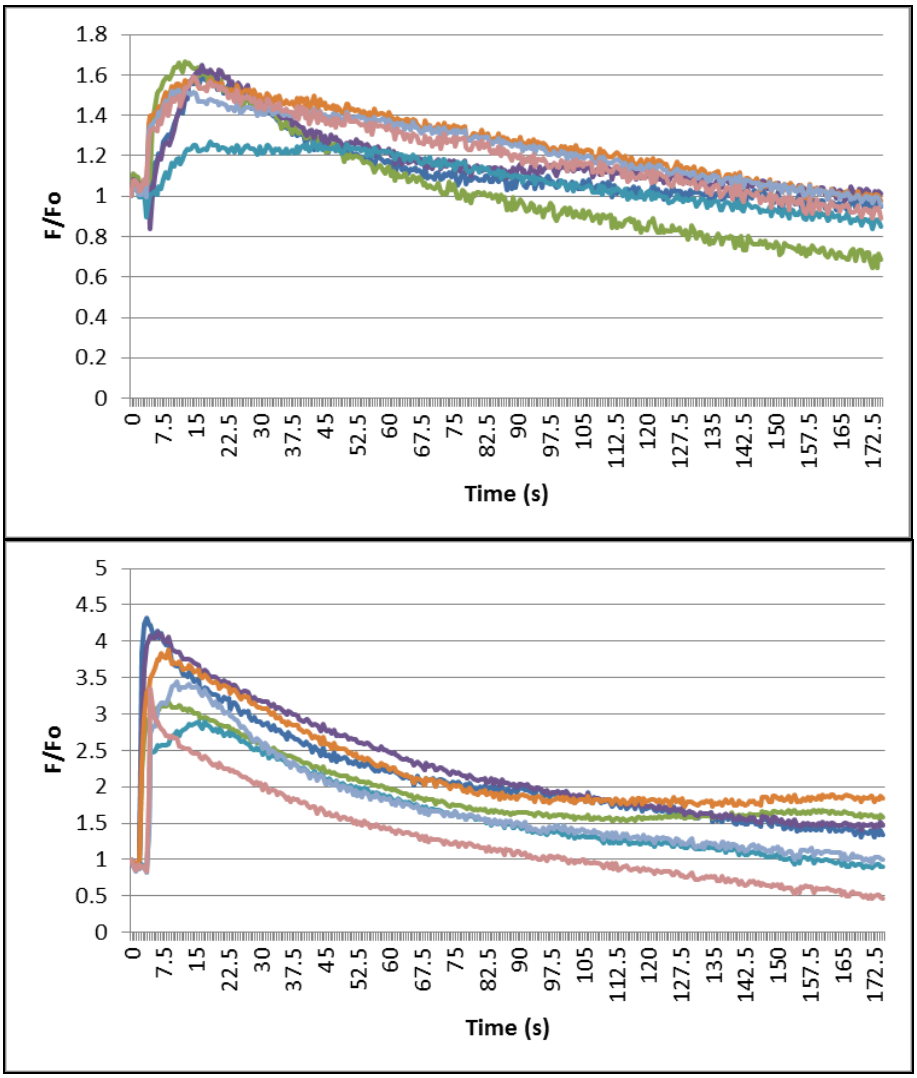

Figure 3.7 Change in calcium indicator fluorescence intensity of stretch injured undifferentiated Schwann cells. *Top*, Averaged Schwann cell stretch injured at 50% strain and 30 s^{-1} strain rate (n = 20 cells). *Bottom*, Averaged Schwann cell stretch injured at 70% strain and 30 s^{-1} strain rate (n = 20 cells). *F*/*Fo* = change in calcium fluorescence over initial fluorescence.

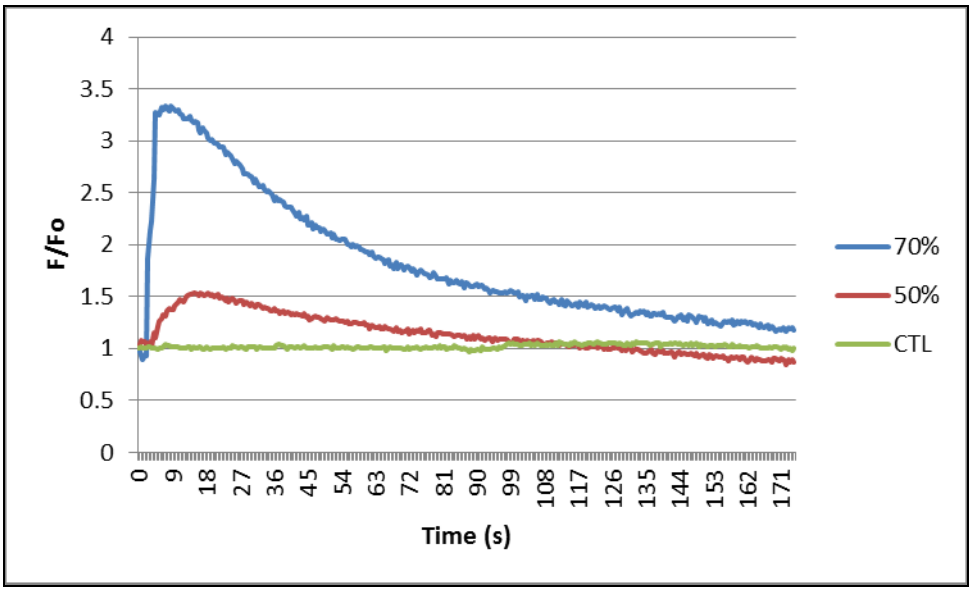

Figure 3.8 The averaged consecutive change in calcium indicator fluorescence intensity over a 3 minute time period; prior, immediately and continuously after stretch injury to undifferentiated schwann cells at 50% and 70% strain at 30 s^{-1} strain rate (n = 8 wells). The averaged fluorescence intensity of non-injured undifferentiated Schwann cells or control experiment (CTL; n = 3 wells). *F*/*Fo* = change in calcium fluorescence over initial fluorescence.

3.2.2 Calcium Response in Uninjured Undifferentiated Schwann Cells

The uninjured Schwann cells are blocked from injury by the dense and unyielding deformation mask and are positioned approximately 5.0 mm away from injury site (Figure 3.9).

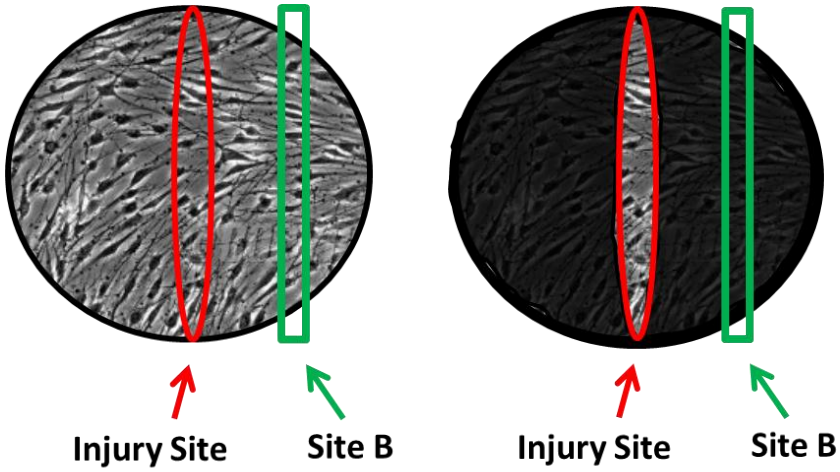

Figure 3.9 Example of undifferentiated Schwann cell culture in an injury well for a stretch injury experiment. Labeled are the stretch injury site as *Injury Site* in red and un-stretched injury site as *Site B* in green. *Right*, shaded region indicates un-stretch injured area.

The un-stretched injured cells in an uninjured culture observed a baseline fluorescence using the calcium indicator fluo-4 ($F/Fo \sim 1$), which concurred an absence of over exposure (Figure 3.11). There was an insignificant flickering of fluorescence in all control experiments. The uninjured Schwann cells had a slight increase in the measured fluorescence immediately after a mild injury and a higher intensity in the severe injury (Severe, $F/Fo = 1.8$; Mild, $F/Fo = 1.2$) (Figure 3.10). This indicated a rise of intracellular calcium concentration following trauma. The averages represent an increase in calcium levels ($F/Fo \geq 1$) to the biological intracellular concentration level

(*F/Fo* ~ 1) (Figure 3.10, 3.11). The basal level was reached post-trauma after a downward trend from the maximum mean fluorescence over a two minute time period.

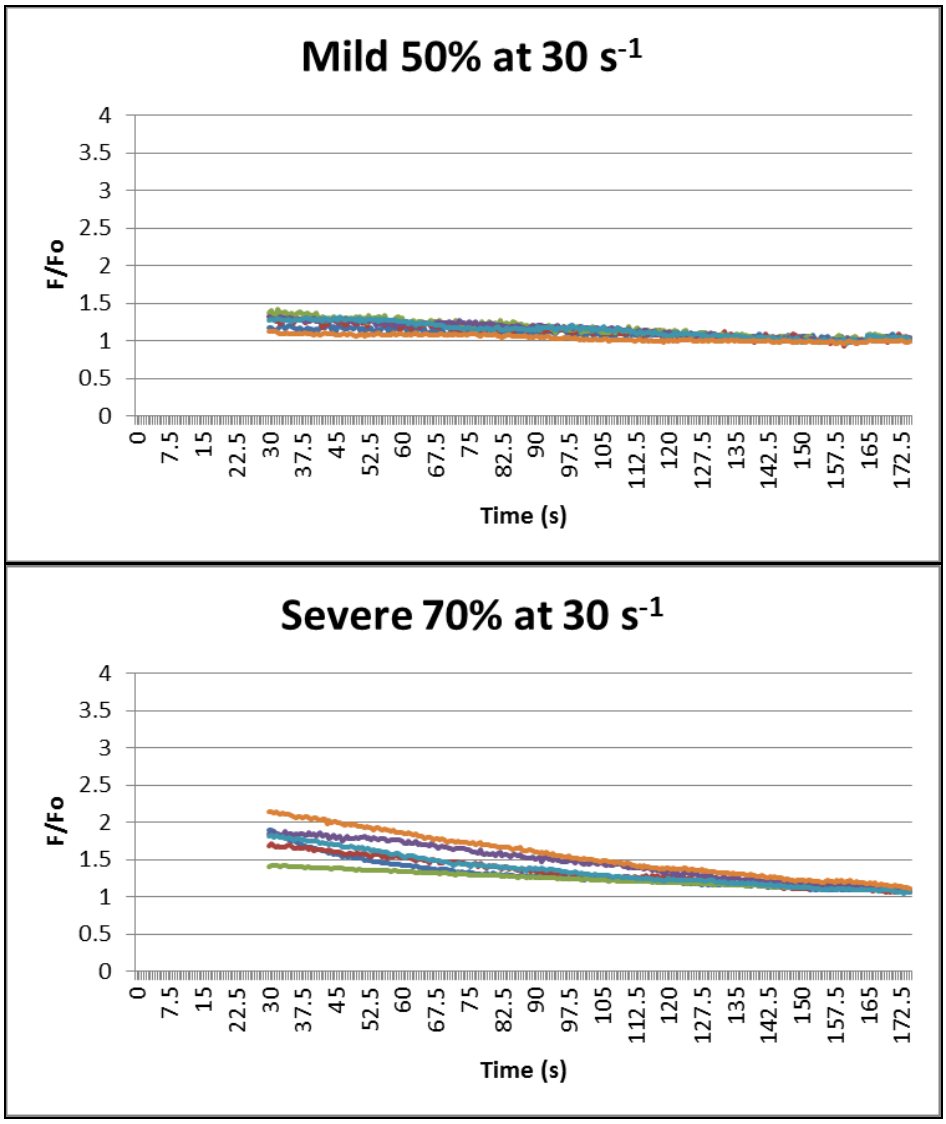

Figure 3.10 Consecutive change in averaged calcium indicator fluorescence intensity of uninjured undifferentiated Schwann cells, isolated away from stretch injury site. The intensity was measured approximately 20-30 seconds after injury. *Top*, Uninjured undifferentiated Schwann cells response to stretch injury at 50% strain at 30 s^{-1} strain rate (n = 20 cells). *Bottom*, Uninjured undifferentiated Schwann cells response to stretch injury at 70% strain at 30 s^{-1} strain rate (n = 20 cells). *F/Fo* = change in calcium fluorescence over initial fluorescence.

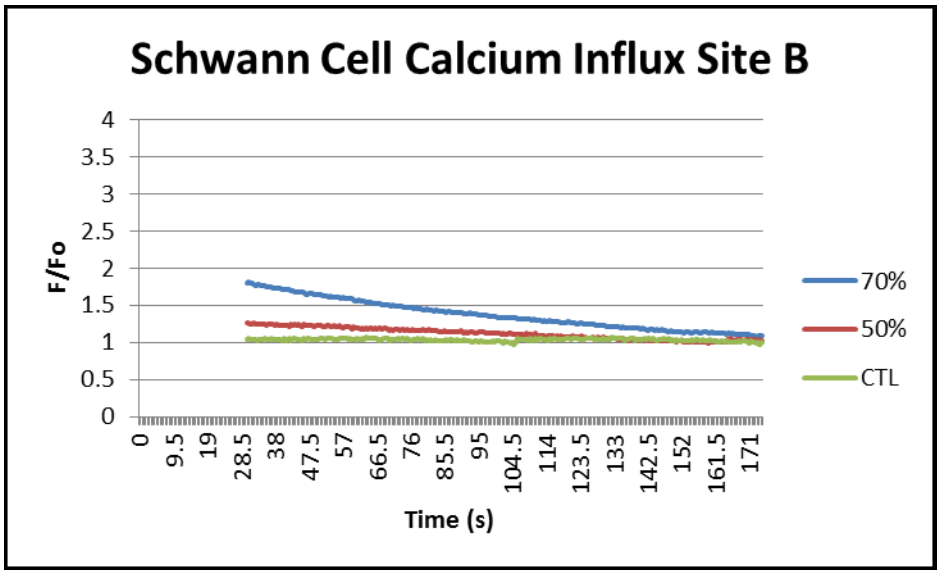

Figure 3.11 Consecutive changes in calcium indicator fluorescence intensity of uninjured undifferentiated Schwann cells, isolated away from stretch injury site, at 50% and 70% strains at 30 s^{-1} strain rate (n = 6 wells). Images were taken approximately 20-30 seconds after injury. The non-injured control (CTL) of uninjured undifferentiated Schwann cells fluorescence intensity was averaged (n = 3 wells). *F*/*Fo* = change in calcium fluorescence over initial fluorescence.

3.2.3 Calcium Response in Differentiated Schwann Cells

The non-injured differentiated Schwann cells showed baseline fluorescence by the fluo-4 fluorescing calcium indicator (*F/Fo* ~ 1). This identified no significant fluctuation in the calcium level. The injured differentiated Schwann cells showed an immediate increase in fluorescence at the time of injury. This corresponded to the increase in intracellular calcium concentration immediately after a severe and mild injury (Figure 3.13) (Severe, *F/Fo* = 3.5; Mild, *F/Fo* = 2.0; subjective measurements). No fluctuation in the intracellular concentration (*F/Fo* ~ 1) to an increase in calcium levels (*F/Fo* ≥ 1) was indicated by the averages (Not Shown). After the post-traumatic baseline response of unaffected cells there was a gradual upward trend in the fluorescence over the next two minutes (Figs. 3.12, 3.13). However, differentiated Schwann cells did not return to baseline following the increased fluorescence, instead they sustained a high level of

fluorescence intensity (Figure 3.13) (t = 2 minutes; Severe, F/Fo = 2.0; Mild, F/Fo = 1.5).

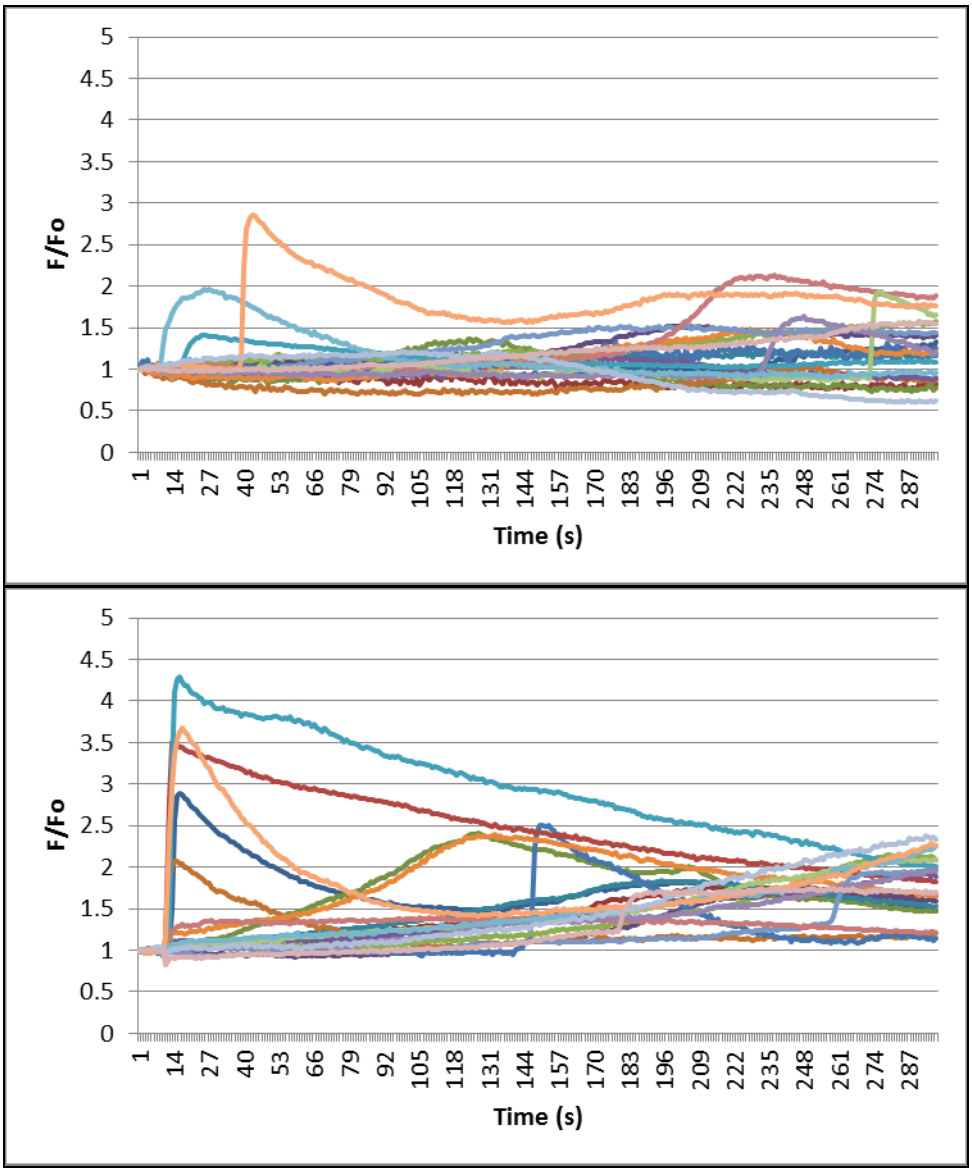

Figure 3.12 Consecutive change in calcium indicator fluorescence measurement for stretch injured differentiate Schwann cells. The fluorescence intensity was measured approximately 3-5 seconds prior to injury. *Top*, Stretch injury at 50% strain at 30 s^{-1} strain rate (n = 1 cell, 20 cells). *Bottom*, Stretch injury at 70% strain at 30 s^{-1} strain rate (n = 1 cell, 20 cells). *F*/*Fo* = change in calcium fluorescence over initial fluorescence.

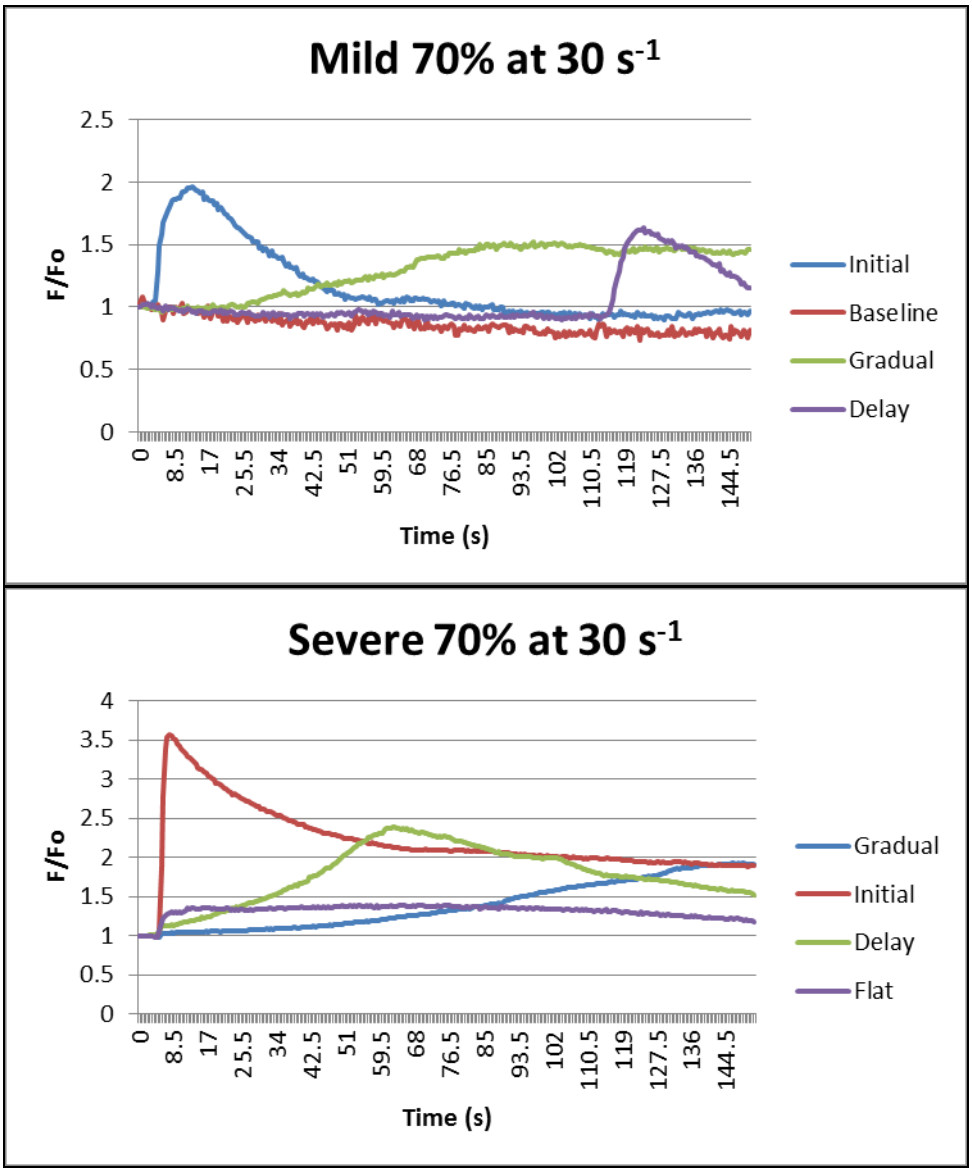

Figure 3.13 Change in measured calcium indicator fluorescence intensity for stretch injury to differentiated Schwann cells. The fluorescence intensity was measured approximately for 3-5 seconds prior to injury and a 3 minutes time period.. *Top*, Stretch injury trends at 50% strain at 30 s^{-1} strain rate (n = 1-5 cells in 6 wells). *Bottom*, Stretch injury trends at 70% strain at 30 s^{-1} strain rate (n = 1-5 cells in 6 wells). *F*/*Fo* = change in calcium fluorescence over initial fluorescence.

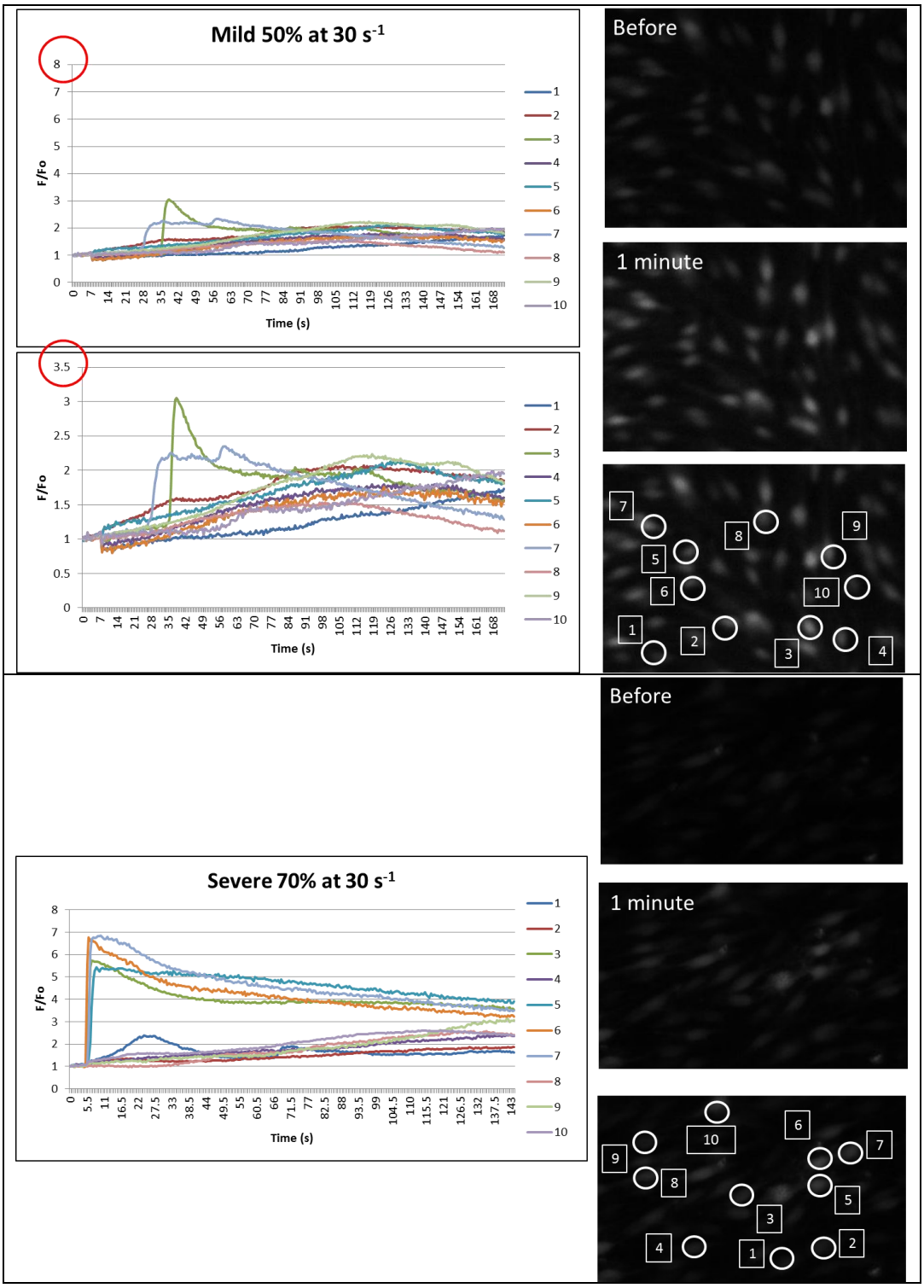

Figure 3.14 Consecutive change in measured calcium indicator fluorescence intensity for stretch injury to differentiate Schwann cells. *Top*, Stretch injury at 50% strain at 30 s^{-1} strain rate (n = 1 cell). *Bottom*, Stretch injury at 70% strain at 30 s^{-1} strain rate (n = 1 cell). *F/Fo* = change in calcium fluorescence over initial fluorescence.

CHAPTER 4

DISCUSSION

4.1 DRG Approach to Stretch Injury

To study the effects of DAI on white matter an *in vitro* stretch injury system, capable of real time viewing, was used to evaluate myelinated axon pathology instantaneously after stretch injury (Magou et al., 2011). Cortical neurons have not been able to remain healthy in culture to support oligodendrocytes, central nervous system (CNS) myelinating glial cells, to myelinate axonal extensions. To overcome this, dorsal root ganglion (DRG), neurons of the peripheral nervous system (PNS), have been shown to myelinate in co-culturing systems with oligodendrocytes (Chan et al., 2004). DRG cultures can last the length in time it will take to grow out axon extensions from embryonic DRGs, co-culture with oligodendrocytes, induce myelination and develop mature myelin. Oligodendrocytes myelination on DRG axons is comparative to myelination on cortical axons (Chan et al., 2004).

4.2 DRG Pathology Induced by Stretch Injury

An *in vitro* experiment is conducted by isolating components of a tissue or organ from their natural biological environment for a more distinct analysis. The overall aim is to first mimic the biopathology of the components *in situ*, demonstrate similar characteristics and then further analyze the underlying pathology and find molecular targets for treatment intervention. A previous stretch injury model applied strains to cortical axons which replicated the mechanical loading experienced by axons *in vivo*

during traumatic brain injury and resulted in the development of multiple swelling along the axons (Smith et al., 1999). The swellings were stated to have a similar appearance of axonal swellings found after DAI in humans (Adams et al., 1989; Povlishock et al., 1992; Smith et al., 1999). The *in vitro* model was therefore determined to be suitable to reproduce the significant pathological feature of traumatic axonal damage found clinically. In the present study, the use of a stretch injury *in vitro* model, capable of viewing and analyzing immediately after the injury, was used to apply scientifically relevant strains to cultured DRG axons. The strains applied to the DRG axons by the stretch injury device resulted in swellings randomly dispersed along the axons (Figure 3.6). This morphology had a similar appearance to beadings along the stretch injured cortical axons *in vitro* (Smith et al., 1999).

Stretch injured DRG axons, using the injury model in the present study, demonstrating the same morphology of stretch injured cortical axons *in vitro* allowed for the further analysis of DRG axon pathology. Axonal DRGs morphologic and physiologic traits which occur immediately after injury were evaluated using the *in vitro* stretch injury model (Magou et al., 2011). Changes to DRG axon morphology and intra-axonal calcium influx after stretch injury were correlated to stretch injured cortical axons (Smith et al., 1999; Wolf et al., 2001).

In the present study, stretch injury on isolated DRG axons led to notable observations. The first, DRG axons have a higher tolerance to strains compared to corticals axons (Smith et al., 1999). Secondly, DRG axons had a delayed recovery similar to what was seen in corticals but a severe injury demonstrated a delay before the axons showed a gradual recovery (Smith et al., 1999). Third, degeneration and axonal

thinning was seen in severe injuries 24 hours after stretch injury. Finally, the rise of intracellular calcium concentration occurred in two phases. The first flux was immediately after injury and mainly due to extracellular entry, but for a severe injury showed intracellular calcium stores release contributing to the calcium concentration increase. The second influx, after intracellular recovery to homeostasis calcium levels from the first influx, had an incremental increase due to a severe injury similar to what was exhibited in cortical axon stretch injury (Wolf et al., 2001).

4.2.1 Axonal Parameters for Stretch Injury

The strains applied to DRG axons were defined by the biopathology characterized in cortical axons after injury. The severity of injury was described as mild or severe injuries, which are distinguished by similarities to the clinical descriptions of minor axonal damage and moderate axonal damage or secondary axotomy in DAI respectively (Povlishock et al., 1992; Maxwell et al., 1993; Povlishock and Christman, 1995). Mild experimental strain values were predefined by characterizing axons post injury with minor damage; temporary impairment, slight occurrence of axonal beading and no fragmentation. In the present study, axonal swellings and no fragmentation were evident after injury (Figure 3.1). This was demonstrated at a strain of 60%. Severe experimental strain values were demonstrated by these characterized descriptions but in addition 24 hours after injury showed the axonal body degenerating as fragmentation and thinning of the axolemma (Figure 3.2); clinically describe in moderate injuries with secondary axotomy occurring hours to days following injury (Maxwell et al., 1993). This was seen at 90% strain for DRG axons demonstrating a high tolerance to the applied strain by the

stretch injury model. Adherence to the substrate and no primary axotomy was evident of the axons in both injury severities.

In the previous research model, cortical axon studies were applied to strains where the axons remained attached to the substrate between 58-65% (Smith et al., 1999). Examination of axons revealed that they experienced strains that corresponded to the underlying substrate until primary axotomy occurred. They determined that the uniaxial strain on the substrate at which primary axotomy could be found was greater than 65%.

The DRG axons were expected to have a greater tolerance to the strain parameters first established by cortical characterization due to the diameter of PNS axons being larger and more robust than the axons in the CNS (Smith et al., 1999; Debanne et al., 2011).

4.2.2 Axonal Delayed Response to Stretch Injury

Stretch injury to DRG axons resulted in the random occurrence of morphological undulations (Figure 3.1, 3.2). The axon body formed undulations from adherence to the deformed membrane correlating the amount of stretch to the membrane to the extent of elongation of the axons. The axons then showed an active recovery in their length and orientation following injury. The gradual recovery of the axonal undulations to their original orientation and length had a linear progression but for a severe injury there was a delay in the recovery (Figure 3.3). This could be rationalized dynamically by a severe injury causing a shocking comprisement to the intracellular structure whose reorganization is paused, becomes acclimated and then restructures itself.

Stretch injury leads to a compromised cytoskeleton, indicated by a perturbed axonal transport and the subsequent accumulation of discharged protein and organelle

cargos viewed externally as regional axonal swellings (Maxwell et al., 1993; Gaetz, 2004; Kilinc et al., 2008). The cytoskeleton is a dynamic structure capable of reorganizing the subunits of the structure (Povlishock and Christman, 1995). The pliability of the cytoskeleton is demonstrated when it acclimates to the curvature of the undulations. This active intracellular structure and the kinetics of its recovery after injury could be a determinant for the subsequent axonal degeneration and fragmentation. There are two notable traits of the axon cytoskeleton in regards to the delayed recovery; (1) The structure is instinctually undiluted, it can not only accommodate the stretch and force but will reorient itself, (2) instead of retaining the stretched length the cytoskeleton will retract.

Smith's results represented the first observation of a delayed response of cortical axons to dynamic deformation from stretch injury (Smith et al., 1999). The delayed response of the axons to mechanical stretch in the study included an increase in length and arbitrary undulations, then the subsequent gradual recovery to their original orientation.

4.2.3 Axonal Degenerative Response to Stretch Injury

Severe injuries to DRG axons demonstrated the biopathology found after stretch injury to cortical axons but were further analyzed 24 hours after stretch injury to determine if the axons showed signs of degeneration. The axons indicated the axonal body degenerating by fragmentation and thinning of the axolemma (Figure 3.2). This is described clinically as happening in secondary axotomy in human with DAI, occurring hours or days after injury (Blumbergs et al., 1989). The consistency of the axon structure 24 hours after injury was verified by the morphological markers of axonal beadings apparent in

degenerating axonal body as globular structures (Maxwell et al., 1993; Maxwell, 1996; Smith et al., 1999).

4.3 Calcium Response in Stretch Injured Axons

It had been inferred the delayed onset of axonal damage was due to detrimental intracellular pathology initiated by heightened levels of calcium concentration in the cell after injury (Maxwell et al., 1993; Gaetz, 2004). The *in vivo* analysis of increased intracellular calcium in injured axons had not been directly demonstrated due to imaging and *in vivo* limitations (He et al., 2005; Wang et al., 2009). An *in vitro* study to cortical axons demonstrated an influx of calcium after stretch injury (Wolf et al., 2001). However, the change in intracellular calcium was looked at 30 seconds after injury. In the present study a calcium increase immediately after injury, approximately half of a second, has not been examined and was shown to be a significant increment of time following injury. The stretch injury model used in the present study measured the intracellular calcium concentration immediately after and subsequent to the DRG axonal stretch injury. The immunofluorescence calcium indicator fluo-4 indicated an immediate increase in intracellular calcium, subsequently returning to homeostasis levels within 30 seconds, followed by a second increase in a severe injury, both of which are dependent on the presence of extracellular calcium.

4.3.1 Two Phases of Calcium Increase

The second flux of intracellular calcium in stretch injured DRG axons showed an incremental increase after a severe injury (Figure 3.5). However, in a mild injury this occurrence was absent and there was no change in the calcium level. This suggested the

severity of injury determines whether there will be a sustained higher level of intracellular calcium continuously after injury. Previous research has indicated damage to the axons causes a rapid influx of extracellular calcium triggering destructive pathology (Maxwell et al., 1993). Intracellular signaling cascades leading to enzyme activation and calcium activated proteases, damaging the intracellular environment, are additive to the development of axonal swellings and to the delayed fragmentation and axonal disconnection (Povlishock et al., 1992; Maxwell et al., 1993; Maxwell, 1996; Matute and Ransom, 2012). This could rationalize why in the present study a mild injury, with an absence of calcium influx after injury, remained vital hours after injury; and accounts for the clinical description of a minor injury having axon revival. Furthermore, a relationship between the sustained high level of calcium and the morphology 24 hours after a severe injury, with fragmentation and axonal thinning, implicates a time sensitive target for pharmaceutical intervention.

In vivo research on post-traumatic calcium accumulation in axons has been indirectly observed. Injury to an optic nerve determined an increase in intercellular calcium in damaged axons (Gennarelli et al., 1989; Maxwell et al., 1995). The ability to examine the mechanism of calcium influx or continuous observation after injury is limited for *in vivo* experiments (Crooks et al., 2007; Wang et al., 2009). The previous *in vitro* stretch injury model demonstrated the increasing calcium levels in stretch injured un-myelinated cortical axons (Wolf et al., 2001). This research postulated the normal calcium buffering ability of axons is overwhelmed after injury.

A calcium increase in cells immediately after injury has not been demonstrated. The *in vitro* model used in the present study allowed the change in calcium levels of

stretch injured DRG axons to be analyzed half of a second after injury. A moderate instantaneous rise in intracellular calcium was indicated immediately after the injury and instantaneously returned to homeostasis intracellular calcium levels (Figure 3.5). The calcium increase immediately after injury could be the cause for the second calcium increase found in a severe injury, but the lack of occurrence in both mild and severe would not support this notion. However, the calcium influx immediately after injury could potentially be the cause for the development of axonal beadings arbitrarily occurring after injury in both severities; demonstrated by the development of the swellings coinciding with the accumulation of calcium in the swellings.

4.3.2 Both Phases of Calcium Influx Depend on Extracellular Calcium

The removal of extracellular calcium, using a calcium free serum (HBSS, no calcium), in a severe injury to DRG axons showed no change in the calcium level following injury. This suggested the influx and sustained high levels of calcium after injury were dependent on extracellular entry. However, immediately after injury there was a slight variance in the level of calcium. For a mild injury it was insignificant but for a severe it was enough to suggest the possible release from the intracellular calcium stores which could be connected to the second influx of calcium.

4.3.3 Mechanism of Calcium Pathology Underlying Axon Stretch Injury

(1) Injury causes calcium influx through plasma membrane

In the present study, the mechanism of calcium entry through the axolemma in the stretch injured DRGs axons could be postulated by equating the entry of calcium into the cortical axons. The previous *in vitro* study on stretch injured cortical axons found that treatment

with tetrodotoxin (TTX) completely blocked calcium influx after stretch injury (Wolf et al., 1999). This suggested the sodium influx through voltage gated sodium channels and an increase in intra-axonal calcium after axonal trauma were related. They further proposed a mechanism of calcium entry into stretch injured axons. First, the strain on the axonal membrane causes an influx of sodium through mechanosensitive sodium channels and second, in response a reversal of axonal sodium-calcium exchangers and activation of voltage gated calcium channels (VGCCs) collectively contributing to a pathological influx of calcium into the axons. In their study they found that treatment of axons with the sodium-calcium exchanger blocker bepridil slightly lowered the influx of calcium after stretch injury. Pretreatment of axons with ω-conotoxin, which blocks P/Q- and N-type VGCCs, significantly decreased the influx of calcium seen in axonal stretch injury.

DRGs have TTX resistant calcium channels so the relationship with sodium influx cannot be insinuated (Yoshimura et al., 2001). However, DRG calcium channels can be block by ω-conotoxin which blocks calcium entry through N-type calcium channels (McDonough et al., 1996). It can therefore be suggested the stretch injury causing depolarization of VGCCs leading to an influx of calcium into the cortical axons by ω-conotoxin sensitive N-type VGCC could have the same mechanistic pathology in stretch injured DRGs axons.

(2) Calcium Ions Release Calcium from Intracellular Stores

The stretch injured DRG axons in the present study could have a direct pathway for the influx of extracellular calcium ions to induce the release of calcium from the intracellular calcium stores immediately after stretch injury. Previous studies showed in DRG neurons the increase in intracellular calcium occurring during cell plasma membrane

depolarization through VGCCs (Shmigol et al., 1995). The calcium induced calcium release (CICR) from internal stores (endoplasmic reticulum; abbreviated ER) by the ryanodine receptors (RyRs) contributes to the calcium increase in neurons (Solovyova et al., 2002). The inhibition of RyRs by caffeine results in a lower increase in intracellular calcium in DRG neurons (Lu et al., 2006). The initial calcium influx by depolarization was shown to occur immediately after stretch injury to cortical axons through VGCCs (Wolf et al., 2001). Therefore the initial calcium influx by depolarization occurring immediately after stretch injury through VGCCs could lead to the calcium release by RyRs from intracellular calcium stores.

(3) Injury Causes Calcium Store Release

The release of calcium from the intracellular calcium stores at the time of stretch injury to the DRG axons could be a calcium-independent event exclusively involving the external mechanical stimulation to the membrane proteins resulting in an intracellular signaling cascade prompting the release of calcium from intracellular stores. Cell and calcium storage organelle membranes are linked by a cell signaling pathway involving intracellular secondary messenger inositol 1,4,5-trisphosphate (IP3) (Lange, 2011). Previous research used the IP3 receptor blocker 2-aminoethoxydiphenylborate (2-APB) to monitor the release of calcium from internal stores. In order to confirm 2-APB blocked IP3 receptor mediated release of calcium an analogous of IP3, uridine-5'-triphosphate (UTP), was used. The application of 2-APB inhibited the increase in intracellular calcium induced by UTP, and concurred an IP3 pathway releasing intracellular calcium stores (Lu et al., 2006). A study indicated a high concentration of IP3 and increased expression of IP3 receptor IP4R1 after hypoxic/reperfusion injury of

spinal cord dorsal column (Kesherwani and Agrawal, 2012). Therefore it could be suggested the opening of intracellular calcium stores is through an IP3-dependent signaling pathway from axonemma ligand stimulation by stretch injury.

4.4 Calcium Response in Stretch Injured Schwann Cells

In the peripheral nerves there are two main cells types, differentiated (myelinating) Schwann cells and undifferentiated (non-myelinating) Schwann cells (Mirsky et al., 2008). Injury has been shown to increase intracellular calcium in Schwann cells (Jahromi et al., 1992). Calcium increase in these cells can be damaging to their viability and the cells around them (Ciutat et al., 1996). However, increased intracellular calcium in glial cells, applied by stretch injury, has not been demonstrated. In the present study the *in vitro* stretch injury system examined changes in intracellular calcium levels of differentiated Schwann cells and undifferentiated Schwann cells. The calcium sensitive dye fluo-4 indicated an increase in calcium levels of both stretch injured Schwann Cells.

The loading conditions for the Schwann cells were correlated to the stretch injured cortical axons because the axonal damage was caused by analogous environment to human brain trauma and therefore the Schwann cells injury in the current model would reflect the expected injury to oligodendrocytes. In the present study the *in vitro* stretch injury model applied severe and mild injury to Schwann cells by strains of 70% and 50% respectively.

4.4.1 Undifferentiated Schwann Cells Response to Stretch Injury

Stretch injury to undifferentiated Schwann cells showed an increase in intracellular calcium levels immediately after injury (Figure 3.7, 3.8). The high calcium concentration

gradually decreased after injury till the homeostasis levels were reached, occurring in both mild and severe injury. The influx of calcium into the undifferentiated Schwann cells could be through voltage gated calcium channels which has been shown *in vivo* to be a dominate entry for the influx of calcium to enter the cell. Few *in vivo* studies have examined calcium accumulation directly in traumatic injured Schwann cells. Robitaille's study indicated calcium entry through VGCCs detected by mechanically stimulated perisynaptic Schwann cells at the frog neuromuscular junction (Robitaille et al., 1996).

4.4.2 Differentiated Schwann Cells Response to Stretch Injury

Differentiated Schwann cells immediately after stretch injury had an increase in intracellular calcium levels which did not reduce completely to homeostasis levels as seen in undifferentiated Schwann cells (Figure 3.12, 3.13, 3.14). This could be due to the calcium ions entering extracellularly into cells and then traversing through cell-cell gap junctions instead of exiting the cell as seen in undifferentiated Schwann cells. Gap junctions are a type of intercellular connection between neighboring cells which directly connects their cytoplasm and allows molecules and ions to intracellularly traverse between them. Differentiated Schwann cells, unlike undifferentiated Schwann cells, have gap junctions. The protein connexin32 (Cx32) is a gap junction protein, which is absent in undifferentiated Schwann cells, and important in the functioning of gap junctions in differentiated Schwann cells (Scherer, 1996). A research study indicated the absence of Cx32 hinders the functional and structural integrity of differentiated Schwann cells, demonstrated in Cx32 knockout mice developing demyelinating neuropathy (Scherer et al., 1998).

The stretch injured differentiated Schwann cells in the present study did not cause all the cells to be injured. Those cells in the injury site, but were not damaged or demonstrating a calcium influx at the time of injury, showed a gradual increase in calcium concentration after injury (Figure 3.14). The increasing calcium levels plateaued at a moderate level slightly above the homeostasis calcium concentration. The non-injured cells with a delayed calcium increase could have had the calcium enter their cells through gap junctions connecting them to injured cells with high calcium levels. The calcium concentration gradient favors traveling from an area with high concentration, as the injured cells, to a lower concentration as the non-injured cells.

4.4.3 Additional Pathway for Intracellular Calcium Increase

(1) Extracellular mechanism:

In the present study, uninjured undifferentiated Schwann cells were isolated from the injured cells and their calcium levels after injury were determined. The uninjured undifferentiated Schwann cells demonstrated the possible release of an extracellular messenger from the injured undifferentiated Schwann cells by their high calcium levels following injury (Figure 3.10, 3.11). In addition, the gradual increase in the injured differentiated Schwann cells, additive to the calcium traversing through gap junctions, could also be due to the release of an excitatory extracellular messenger from injured cells to the non-injured cells.

Research has shown evidence of extracellular signaling molecules being released from injured Schwann cells and influencing the calcium levels in others cells. Experiments on squid axons demonstrated nerve stimulation triggering a hyperpolarization of periaxonal Schwann cells was mimicked by glutamate, a major

excitatory neurotransmitter, and blocked by a glutamate antagonist (Lieberman et al., 1989; Lieberman, 1991). Another study showed dissociated Schwann cells from neonatal rat scitoatic nerves responding to glutamate by an increase in their intracellular calcium levels (Lyons et al., 1994). Release of glutamate from Schwann cells in organotypic cultures has been shown to be due to a rise in intracellular calcium concentration (Parpura et al., 1995). Therefore the rise of intracellular calcium at the time of injury could cause the release of an extracellular signaling molecule, such as glutamate, to increase the calcium level in uninjured cells.

CHAPTER 5

CONCLUSIONS

5.1 Coculture Signaling Between Axons and Schwann Cells

Demyelination has been postulated to be caused by a signaling pathway from axons to myelin forming Schwann cells following traumatic injury. The degeneration of a myelinated axon is initiated by a signaling pathway commencing from an injured axon to the encapsulating Schwann cell. A study showed the stacking of myelinating Schwann cells on an axon protects the outer myelin sheath from degeneration (Kidd and Heath, 1991). Demonstrating contact between myelin and axon is required for this pathology and there is a signaling event taking place. Signaling factors have been established to occur in the close contact signaling between axons and the myelin sheath in the peripheral nervous system. Neuregulin, when added to a co-culture of myelinated DRGs by Schwann cells, induced demyelination by Schwann cell dedifferentiation and proliferation (Chen et al., 1994; Zanazzi et al., 2001).

5.2 Coculture Signaling Between Axon and Oligodendrocytes

External stimulus to neurons has been shown to influence intracellular calcium signals in myelinating cells. These cells intracellular calcium levels increase and in mechanistically ill-defined way affect the neurons calcium levels. White matter neuronal activity has been shown *in vivo* to increase intracellular calcium in glial cells (Verkhratsky et al., 1998). An experiment demonstrated electrical stimulus by oscillations to the optic nerve causes oscillations in the intracellular calcium level of oligodendrocytes (Kriegler and

Chiu, 1993). Some studies have looked at possible neurotransmitter initiators. Certain channels and associated neurotransmitters, such as the glutamate transporter and the glutamate neurotransmitter, have been hypothesized to be the components involved in neuronal signaling which alter intracellular calcium levels in glial cells in the white matter of the brain. High levels of glutamate cause excitotoxicity in neurons and oligodendrocytes (Choi, 1992; Oka et al., 1993). White matter nerve fiber tracts in certain mammals and frogs have been shown to release glutamate during electrical stimulation (Wheeler et al., 1966; Weinreich and Hammerschlag, 1975). The release of signaling molecules from damaged axons, such as glutamate, occurs after TBI (Obrenovitch et al., 1997).

5.3 Similar Signaling Mechanism of Myelinating Glial Cells

The release of a signaling molecule from an injured neuron was postulated to cause Wallerian degeneration or degradation of myelin proteins. The molecule is unknown but it was proposed to originate from the plasma membrane of neurons soon after injury. A study showed the stacking of myelinating Schwann cells on an axon, described as a behavior of doubly myelinating Schwann cells, protected the outer myelin sheath from degeneration (Kidd and Heath, 1991). The displacement of a myelinated Schwann cell from axonal contact protected it from myelin breakdown during Wallerian degeneration. In the CNS oligodendrocytes have not been shown to encounter a stacking behavior when myelinating an axon and they do not form gap junction between their cell types but it can be proposed there is an association between them and axons that causes myelin

degeneration and correlates the behavior of demyelination distally along the axon as seen in the peripheral nervous system myelinating glial cells (Orthmann-Murphy et al., 2008).

5.4 Final Statements

The results from the present study suggest myelin degeneration after injury could be due to the delayed myelinating cell death. Increased and sustained high calcium levels in cells following injury are toxic and induce cell death. In this study differentiated (myelinating) Schwann cells sustaining high levels of intracellular calcium after stretch injury was postulated to be due to the gap junction pathway of calcium ion movement or the intracellular calcium increase induced by the release of an extracellular molecule from injured cells.

Another consideration is secondary axotomy causing myelin degeneration either by the failure of the degenerating axon to support glial cell myelination or by the release of calcium from the injured axon increasing the calcium levels in the myelinating glial cell. In the present study, there were sustained high levels of calcium following axonal stretch injury which could correlate to the axon degeneration indicated by fragmentation and axonal thinning of the axons occurring 24 hours after a severe injury.

In summary, these results are the first to show intracellular calcium accumulation in Schwann cells and DRG axons immediately after injury. Also, there is a possible correlation between high sustained levels in stretch injured axons and their degeneration by fragmentation and axonal thinning. The pathology of detrimental intracellular dependent calcium mechanisms and injury induced intracellular mechanisms are possible

targets for pharmaceutical intervention which could be further analyzed by these experiments and the stretch injury model used in this research.

REFERENCES

Adams JH (1992) Head injury. New York, NY: Oxford University Press 5:106-152.

Adams JH, Doyle D, Ford I, Gennarelli TA, Graham DI, McLellan DR (1989) Diffuse axonal injury in head injury: definition, diagnosis and grading. Histopathology 15:49-59.

Adams JH, Graham DI, Murray LS, Scott G (1982) Diffuse axonal injury due to nonmissile head injury in humans: an analysis of 45 cases. Annals of neurology 12:557-563.

Barkovich AJ (2005) Magnetic resonance techniques in the assessment of myelin and myelination. Journal of inherited metabolic disease 28:311-343.

Barrett JN, Magleby KL, Pallotta BS (1982) Properties of single calcium-activated potassium channels in cultured rat muscle. The Journal of physiology 331:211-230.

Blumbergs PC, Jones NR, North JB (1989) Diffuse axonal injury in head trauma. Journal of neurology, neurosurgery, and psychiatry 52:838-841.

Bramlett HM, Dietrich WD (2004) Pathophysiology of cerebral ischemia and brain trauma: similarities and differences. Journal of cerebral blood flow and metabolism : official journal of the International Society of Cerebral Blood Flow and Metabolism 24:133-150.

Brockes JP, Fields KL, Raff MC. 1979. Studies on cultured rat Schwann cells. I. Establishment of purified populations from cultures of peripheral nerve. Brain research 165: 105-18

Bunge MB, Bunge RP, Ris H (1961) Ultrastructural study of remyelination in an experimental lesion in adult cat spinal cord. The Journal of biophysical and biochemical cytology 10:67-94.

Bunge RP, Bunge MB, Bates M (1989) Movements of the Schwann cell nucleus implicate progression of the inner (axon-related) Schwann cell process during myelination. The Journal of cell biology 109:273-284.

Chan JR, Watkins TA, Cosgaya JM, Zhang C, Chen L, et al. 2004. NGF controls axonal receptivity to myelination by Schwann cells or oligodendrocytes. Neuron 43: 183-91

Chen MS, Bermingham-McDonogh O, Danehy FT, Jr., Nolan C, Scherer SS, Lucas J, Gwynne D, Marchionni MA (1994) Expression of multiple neuregulin transcripts in postnatal rat brains. The Journal of comparative neurology 349:389-400.

Choi DW (1992) Excitotoxic cell death. Journal of neurobiology 23:1261-1276.

Choi I, Chiu SY (1997) Expression of high-affinity neuronal and glial glutamate transporters in the rat optic nerve. Glia 20:184-192.

Ciutat D, Caldero J, Oppenheim RW, Esquerda JE (1996) Schwann cell apoptosis during normal development and after axonal degeneration induced by neurotoxins in the chick embryo. The Journal of neuroscience : the official journal of the Society for Neuroscience 16:3979-3990.

Crooks CY, Zumsteg JM, Bell KR (2007) Traumatic brain injury: a review of practice management and recent advances. Physical medicine and rehabilitation clinics of North America 18:681-710, vi.

Crowe MJ, Bresnahan JC, Shuman SL, Masters JN, Beattie MS (1997) Apoptosis and delayed degeneration after spinal cord injury in rats and monkeys. Nature medicine 3:73-76.

Debanne D, Campanac E, Bialowas A, Carlier E, Alcaraz G (2011) Axon physiology. Physiological reviews 91:555-602.

Felts PA, Smith KJ. 1992. Conduction properties of central nerve fibers remyelinated by Schwann cells. Brain research 574: 178-92.

Fillipin LI, Mauriz JL, Vedovelli K, Moreira AJ, Zettler CG, Lech O, Marroni NP, Gonzalez-Gallego J (2005) Low-level laser therapy (LLLT) prevents oxidative stress and reduces fibrosis in rat traumatized Achilles tendon. Lasers in surgery and medicine 37:293-300.

Gaetz M (2004) The neurophysiology of brain injury. Clinical neurophysiology : official journal of the International Federation of Clinical Neurophysiology 115:4-18.

Gennarelli TA, Graham DI (1998) Neuropathology of the Head Injuries. Seminars in clinical neuropsychiatry 3:160-175.

Gennarelli TA, Thibault LE, Adams JH, Graham DI, Thompson CJ, Marcincin RP (1982) Diffuse axonal injury and traumatic coma in the primate. Annals of neurology 12:564-574.

Gennarelli TA, Thibault LE, Tipperman R, Tomei G, Sergot R, Brown M, Maxwell WL, Graham DI, Adams JH, Irvine A, et al. (1989) Axonal injury in the optic nerve: a model simulating diffuse axonal injury in the brain. Journal of neurosurgery 71:244-253.

Geren BB, Schmitt FO (1954) The Structure of the Schwann Cell and Its Relation to the Axon in Certain Invertebrate Nerve Fibers. Proceedings of the National Academy of Sciences of the United States of America 40:863-870.

Ghajar J (2000) Traumatic brain injury. Lancet 356:923-929.

Graham DI (1996) Blunt head injury: prospects for improved outcome. Neuropathology and applied neurobiology 22:505-509.

Guertin AD, Zhang DP, Mak KS, Alberta JA, Kim HA (2005) Microanatomy of axon/glial signaling during Wallerian degeneration. The Journal of neuroscience : the official journal of the Society for Neuroscience 25:3478-3487.

Hartline DK, Colman DR (2007) Rapid conduction and the evolution of giant axons and myelinated fibers. Current biology : CB 17:R29-35.

He Z, Crook JE, Meschia JF, Brott TG, Dickson DW, McKinney M (2005) Aging blunts ischemic-preconditioning-induced neuroprotection following transient global ischemia in rats. Current neurovascular research 2:365-374.

Holboum AHS (1943) Mechanics of Head Injuries. Lancet 2:438-441.

Huxley AF, Stampfli R (1949) Evidence for saltatory conduction in peripheral myelinated nerve fibres. The Journal of physiology 108:315-339.

Jahromi BS, Robitaille R, Charlton MP (1992) Transmitter release increases intracellular calcium in perisynaptic Schwann cells in situ. Neuron 8:1069-1077.

Kerschensteiner M, Schwab ME, Lichtman JW, Misgeld T (2005) In vivo imaging of axonal degeneration and regeneration in the injured spinal cord. Nature medicine 11:572-577.

Kesherwani V, Agrawal SK (2012) Regulation of inositol 1,4,5-triphosphate receptor, type 1 (IP3R1) in hypoxic/reperfusion injury of white matter. Neurological research 34:504-511.

Kidd GJ, Heath JW (1991) Myelin sheath survival following axonal degeneration in doubly myelinated nerve fibers. The Journal of neuroscience : the official journal of the Society for Neuroscience 11:4003-4014.

Kilinc D, Gallo G, Barbee KA (2008) Mechanically-induced membrane poration causes axonal beading and localized cytoskeletal damage. Experimental neurology 212:422-430.

Kriegler S, Chiu SY (1993) Calcium signaling of glial cells along mammalian axons. The Journal of neuroscience : the official journal of the Society for Neuroscience 13:4229-4245.

Lange K (2011) Fundamental role of microvilli in the main functions of differentiated cells: Outline of an universal regulating and signaling system at the cell periphery. Journal of cellular physiology 226:896-927.

Le Bihan D, Mangin JF, Poupon C, Clark CA, Pappata S, Molko N, Chabriat H (2001) Diffusion tensor imaging: concepts and applications. Journal of magnetic resonance imaging : JMRI 13:534-546.

Li Y, Zhang L, Kallakuri S, Zhou R, Cavanaugh JM (2011) Quantitative relationship between axonal injury and mechanical response in a rodent head impact acceleration model. Journal of neurotrauma 28:1767-1782.

Lieberman EM (1991) Role of glutamate in axon-Schwann cell signaling in the squid. Annals of the New York Academy of Sciences 633:448-457.

Lieberman EM, Abbott NJ, Hassan S (1989) Evidence that glutamate mediates axon-to-Schwann cell signaling in the squid. Glia 2:94-102.

Lingor P, Koch JC, Tonges L, Bahr M (2012) Axonal degeneration as a therapeutic target in the CNS. Cell and tissue research 349:289-311.

Lu SG, Zhang X, Gold MS (2006) Intracellular calcium regulation among subpopulations of rat dorsal root ganglion neurons. The Journal of physiology 577:169-190.

Lyons SA, Morell P, McCarthy KD (1994) Schwann cells exhibit P2Y purinergic receptors that regulate intracellular calcium and are up-regulated by cyclic AMP analogues. Journal of neurochemistry 63:552-560.

Maas AI, Stocchetti N, Bullock R (2008) Moderate and severe traumatic brain injury in adults. Lancet neurology 7:728-741.

Magou GC, Guo Y, Choudhury M, Chen L, Hususan N, Masotti S, Pfister BJ (2011) Engineering a high throughput axon injury system. Journal of neurotrauma 28:2203-2218.

Margulies SS, Thibault LE, Gennarelli TA (1990) Physical model simulations of brain injury in the primate. Journal of biomechanics 23:823-836.

Marmarou A, Foda MA, van den Brink W, Campbell J, Kita H, Demetriadou K (1994) A new model of diffuse brain injury in rats. Part I: Pathophysiology and biomechanics. Journal of neurosurgery 80:291-300.

Matute C, Ransom BR (2012) Roles of white matter in central nervous system pathophysiologies. ASN neuro 4:89-101.

Maxwell WL (1996) Histopathological changes at central nodes of Ranvier after stretch-injury. Microscopy research and technique 34:522-535.

Maxwell WL, McCreath BJ, Graham DI, Gennarelli TA (1995) Cytochemical evidence for redistribution of membrane pump calcium-ATPase and ecto-Ca-ATPase activity, and calcium influx in myelinated nerve fibres of the optic nerve after stretch injury. Journal of neurocytology 24:925-942.

Maxwell WL, Watt C, Graham DI, Gennarelli TA (1993) Ultrastructural evidence of axonal shearing as a result of lateral acceleration of the head in non-human primates. Acta neuropathologica 86:136-144.

McDonough SI, Swartz KJ, Mintz IM, Boland LM, Bean BP (1996) Inhibition of calcium channels in rat central and peripheral neurons by omega-conotoxin MVIIC. The Journal of neuroscience : the official journal of the Society for Neuroscience 16:2612-2623.

Mirsky R, Woodhoo A, Parkinson DB, Arthur-Farraj P, Bhaskaran A, Jessen KR (2008) Novel signals controlling embryonic Schwann cell development, myelination and dedifferentiation. Journal of the peripheral nervous system : JPNS 13:122-135.

Nakagawa T, Zhu H, Morishima N, Li E, Xu J, Yankner BA, Yuan J (2000) Caspase-12 mediates endoplasmic-reticulum-specific apoptosis and cytotoxicity by amyloid-beta. Nature 403:98-103.

Obrenovitch TP, Urenjak J, Zilkha E (1997) Effects of increased extracellular glutamate levels on the local field potential in the brain of anaesthetized rats. British journal of pharmacology 122:372-378.

Oka A, Belliveau MJ, Rosenberg PA, Volpe JJ (1993) Vulnerability of oligodendroglia to glutamate: pharmacology, mechanisms, and prevention. The Journal of neuroscience : the official journal of the Society for Neuroscience 13:1441-1453.

Orthmann-Murphy JL, Abrams CK, Scherer SS (2008) Gap junctions couple astrocytes and oligodendrocytes. Journal of molecular neuroscience : MN 35:101-116.

Parpura V, Liu F, Jeftinija KV, Haydon PG, Jeftinija SD (1995) Neuroligand-evoked calcium-dependent release of excitatory amino acids from Schwann cells. The Journal of neuroscience : the official journal of the Society for Neuroscience 15:5831-5839.

Peerless SJ, Rewcastle NB (1967) Shear injuries of the brain. Canadian Medical Association journal 96:577-582.

Povlishock JT, Becker DP, Cheng CL, Vaughan GW. 1983. Axonal change in minor head injury. Journal of neuropathology and experimental neurology 42: 225-42.

Povlishock JT, Christman CW (1995) The pathobiology of traumatically induced axonal injury in animals and humans: a review of current thoughts. Journal of neurotrauma 12:555-564.

Povlishock JT, Erb DE, Astruc J (1992) Axonal response to traumatic brain injury: reactive axonal change, deafferentation, and neuroplasticity. Journal of neurotrauma 9 Suppl 1:S189-200.

Raff MC, Whitmore AV, Finn JT (2002) Axonal self-destruction and neurodegeneration. Science 296:868-871.

Robitaille R, Bourque MJ, Vandaele S (1996) Localization of L-type Ca^{2+} channels at perisynaptic glial cells of the frog neuromuscular junction. The Journal of neuroscience : the official journal of the Society for Neuroscience 16:148-158.

Ruiz A, Matute C, Alberdi E (2010) Intracellular Ca^{2+} release through ryanodine receptors contributes to AMPA receptor-mediated mitochondrial dysfunction and ER stress in oligodendrocytes. Cell death & disease 1:e54.

Salzer JL (1997) Clustering sodium channels at the node of Ranvier: close encounters of the axon-glia kind. Neuron 18:843-846.

Scherer SS (1996) Molecular specializations at nodes and paranodes in peripheral nerve. Microscopy research and technique 34:452-461.

Scherer SS, Xu YT, Nelles E, Fischbeck K, Willecke K, Bone LJ (1998) Connexin32-null mice develop demyelinating peripheral neuropathy. Glia 24:8-20.

Shmigol A, Verkhratsky A, Isenberg G (1995) Calcium-induced calcium release in rat sensory neurons. The Journal of physiology 489 (Pt 3):627-636.

Shuman SL, Bresnahan JC, Beattie MS (1997) Apoptosis of microglia and oligodendrocytes after spinal cord contusion in rats. Journal of neuroscience research 50:798-808.

Smith DH, Wolf JA, Lusardi TA, Lee VM, Meaney DF (1999) High tolerance and delayed elastic response of cultured axons to dynamic stretch injury. The Journal of neuroscience : the official journal of the Society for Neuroscience 19:4263-4269.

Solovyova N, Veselovsky N, Toescu EC, Verkhratsky A (2002) Ca^{2+} dynamics in the lumen of the endoplasmic reticulum in sensory neurons: direct visualization of Ca^{2+}-induced Ca^{2+} release triggered by physiological Ca^{2+} entry. The EMBO journal 21:622-630.

Stankoff B, Wang Y, Bottlaender M, Aigrot MS, Dolle F, Wu C, Feinstein D, Huang GF, Semah F, Mathis CA, Klunk W, Gould RM, Lubetzki C, Zalc B (2006) Imaging of CNS myelin by positron-emission tomography. Proceedings of the National Academy of Sciences of the United States of America 103:9304-9309.

Stone JR, Okonkwo DO, Dialo AO, Rubin DG, Mutlu LK, Povlishock JT, Helm GA (2004) Impaired axonal transport and altered axolemmal permeability occur in distinct populations of damaged axons following traumatic brain injury. Experimental neurology 190:59-69.

Strich SJ (1961) Shearing of nerve fibres as a cause of brain damage due to head injury. Lancet 443-448.

Tang-Schomer MD, Patel AR, Baas PW, Smith DH. 2010. Mechanical breaking of microtubules in axons during dynamic stretch injury underlies delayed elasticity, microtubule disassembly, and axon degeneration. FASEB journal : official publication of the Federation of American Societies for Experimental Biology 24: 1401-10

Teasdale G, Jennett B (1974) Assessment of coma and impaired consciousness. A practical scale. Lancet 2:81-84.

Trump BF, Berezesky IK (1995) Calcium-mediated cell injury and cell death. FASEB journal : official publication of the Federation of American Societies for Experimental Biology 9:219-228.

Verkhratsky A, Orkand RK, Kettenmann H (1998) Glial calcium: homeostasis and signaling function. Physiological reviews 78:99-141.

Wang J, Hamm RJ, Povlishock JT (2011) Traumatic axonal injury in the optic nerve: evidence for axonal swelling, disconnection, dieback, and reorganization. Journal of neurotrauma 28:1185-1198.

Wang Y, Wu C, Caprariello AV, Somoza E, Zhu W, Wang C, Miller RH (2009) In vivo quantification of myelin changes in the vertebrate nervous system. The Journal of neuroscience : the official journal of the Society for Neuroscience 29:14663-14669.

Weber JT (2012) Altered calcium signaling following traumatic brain injury. Frontiers in pharmacology 3:60.

Weinreich D, Hammerschlag R (1975) Nerve impulse-enhanced release of amino acids from non-synaptic regions of peripheral and central nerve trunks of bullfrog. Brain research 84:137-142.

Wheeler DD, Boyarsky LL, Brooks WH (1966) The release of amino acids from nerve during stimulation. Journal of cellular physiology 67:141-147.

Wilson JT, Pettigrew LE, Teasdale GM (1998) Structured interviews for the Glasgow Outcome Scale and the extended Glasgow Outcome Scale: guidelines for their use. Journal of neurotrauma 15:573-585.

Wolf JA, Stys PK, Lusardi T, Meaney D, Smith DH (2001) Traumatic axonal injury induces calcium influx modulated by tetrodotoxin-sensitive sodium channels. The Journal of neuroscience : the official journal of the Society for Neuroscience 21:1923-1930.

Yaghmai A, Povlishock J (1992) Traumatically induced reactive change as visualized through the use of monoclonal antibodies targeted to neurofilament subunits. Journal of neuropathology and experimental neurology 51:158-176.

Yoshimura N, Seki S, de Groat WC (2001) Nitric oxide modulates Ca(2+) channels in dorsal root ganglion neurons innervating rat urinary bladder. Journal of neurophysiology 86:304-311.

Zanazzi G, Einheber S, Westreich R, Hannocks MJ, Bedell-Hogan D, Marchionni MA, Salzer JL (2001) Glial growth factor/neuregulin inhibits Schwann cell myelination and induces demyelination. The Journal of cell biology 152:1289-1299.

Zimmerman RA, Bilaniuk LT, Genneralli T (1978) Computed tomography of shearing injuries of the cerebral white matter. Radiology 127:393-396.